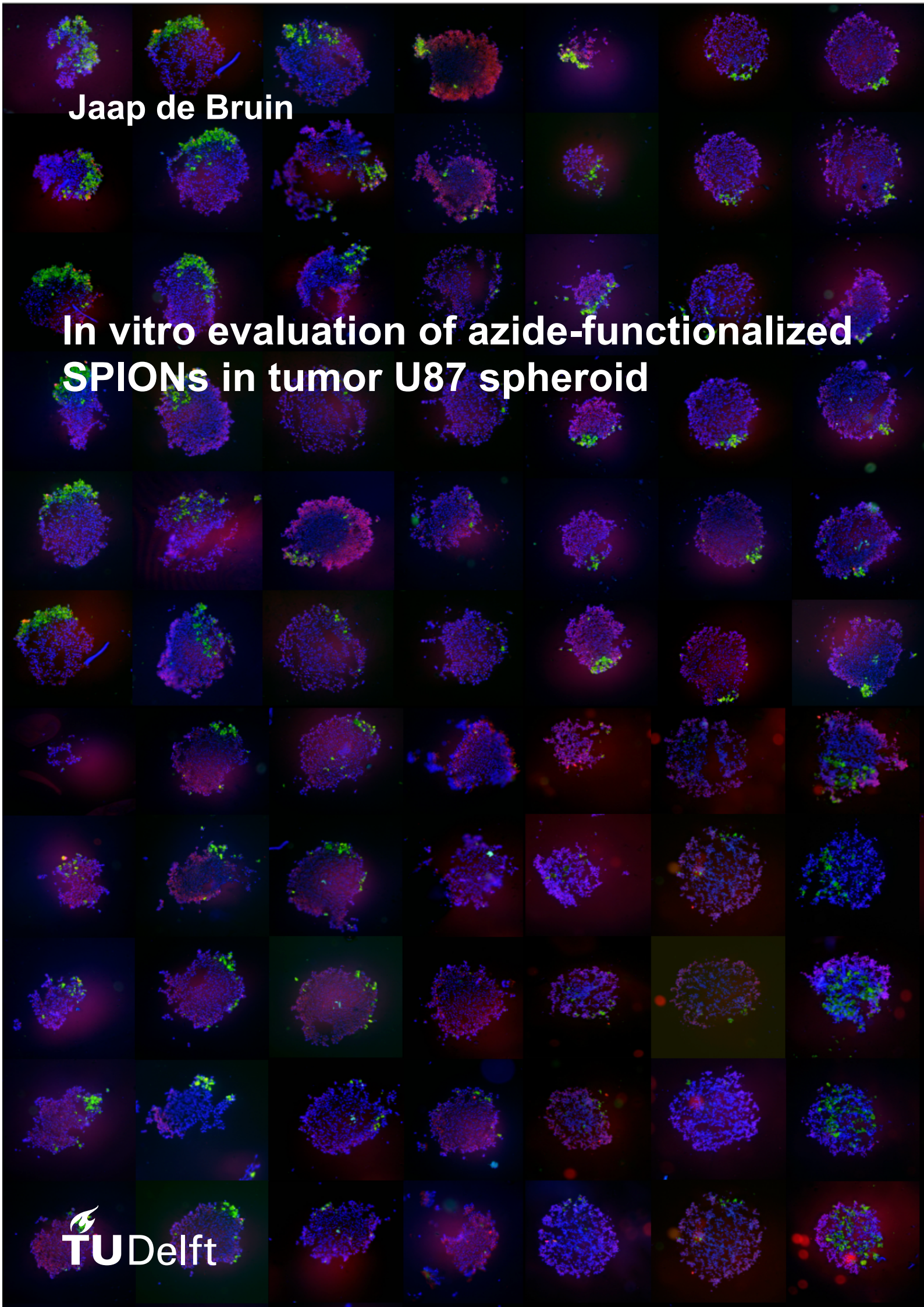

Jaap de Bruin

In vitro evaluation of azide-functionalized SPIONs in tumor U87 spheroid

TU Delft

In vitro evaluation of azide-functionalized SPIONs in tumor U87 spheroid

By

Jaap de Bruin

4721322

in partial fulfilment of the requirements for the degree of

Bachelor of Science
in Molecular Science and Technology

at the Delft University of Technology,
to be defended publicly on Wednesday June 3, 2021 at 03:00 PM.

Supervisor:	Dr. K. Djanashvili	TU Delft/BT
Daily supervisor	R. P. Fauzia	TU Delft/BT
Thesis committee:	Dr. K. Djanashvili	TU Delft/BT
	Dr. Ir. A. G. Denkova	TU Delft/RST

Abstract

Cancer is still one of the most serious diseases for humanity. Internal radiation therapy with alpha particles is a promising method to battle cancer, but it is currently limited to easily accessible tumors. A more advanced and selective method for alpha radiation therapy that will have better outcomes, fewer side effects, and higher efficacy is needed. A promising alternative is a two-step approach in which super paramagnetic iron oxide nanoparticles (SPION's) are first delivered to the cancer cells and then receive the radiotherapeutics in a targeted manner. One of the most important conditions for this strategy is retention of SPIONs at the cell membranes in order to ensure in vivo click-reaction between the azide-functionalized nanoparticles and cyclooctyne-conjugated radiotracer.

The goal of this study is to observe the behavior of two types of SPION's on the glioblastoma multiforme (GBM) cancer cell line U87 and to verify whether the nanoparticles are internalized by the cancer cells or stay on the outside of the membrane. This has been done by growing U87 spheroids, incubating them with the nanoparticles, performing a cryosection on these spheroids, photographing the slices of the cryosection with a fluorescence microscope and analyzing the iron-content of the slices with inductively coupled plasma optical emission spectrometry (ICP-OES). The second part of the study concerns the preliminary in vitro click-reaction of the nanoparticles by adding beta emitter ^{177}Lu coupled to DOTA-cyclooctyne complex to spheroids that were incubated with the nanoparticles.

The fluorescence microscope analysis concludes that the nanoparticles functionalized with polyethylene glycol (PEG) penetrate the U87 spheroids less than the nanoparticles without PEG. The azide click reaction between the nanoparticles and ^{177}Lu-DOTA-cyclooctyne complex was observed and showed more cell damage to the spheroid incubated with nanoparticles then the spheroids that were only treated with ^{177}Lu-DOTA-cyclooctyne.

Contents

Abbreviations and acronyms

Abbreviation	Definition
DMEM	Dulbecco's Modified Eagle Medium
EPR	Enhanced permeability and retention
FA	Folic acid
FBS	Fetal Bovine Serum
Fe	Iron
FITC	Fluorescein isothiocyanate
ICP-OES	Inductively coupled plasma – optical emission spectrometry
^{177}Lu	Lutetium-177
MQ	Milli-Q
MRI	Magnetic resonance imaging
PBS	Phosphate buffered saline
PEG	Polyethyleenglycol
SPION	Super paramagnetic iron oxide nanoparticle

1 Introduction

Cancer is still one of the most serious diseases for humanity: in 2020 it was estimated that there were 19,3 million new cancer cases and 10 million cancer deaths worldwide (Sung, 2021). This makes cancer globally the second leading cause of dead after cardio-vascular diseases (WHO, 2021). New treatments like hormone, immune, photodynamic and photothermal therapies are showing promising results in pre-clinical studies, but surgery, radiation and chemotherapy are still the most common treatments (Arruebo, 2011). These treatments fail, however, to control metastatic cancers to spread through the human body and are highly non-specific in delivering the drugs into cancer cells, which results in undesirable side-effects to healthy tissues and organs (Kumari, 2015).

Internal radiation therapy is promising as it works by damaging the genes in the cancer cells in the form of DNA strands breaks, either by directly ionizing the genes or indirectly by forming free radicals that damage the genes (Hur, 2017). Genes control how the cells grow and divide. The cells that are affected by radiation cannot grow and divide anymore, which results in apoptosis (Figure 1) (American Cancer Society, 2014). Internal radiation therapy uses targeting agents such as antibodies or small molecules tot deliver radiation to the area that needs to be treated. This can be done with radionuclides emitting alpha and beta particles. Beta particles have a longer range and lower energy transfer, which can cause side-effects to non-targeted cells (Medicalexpress, 2019). Alpha particles have higher energy and shorter range, this allows the alpha particles to deliver a cytotoxic effect to a small cell area while limiting the effect on the cells that are not targeted (Solini, 2020).

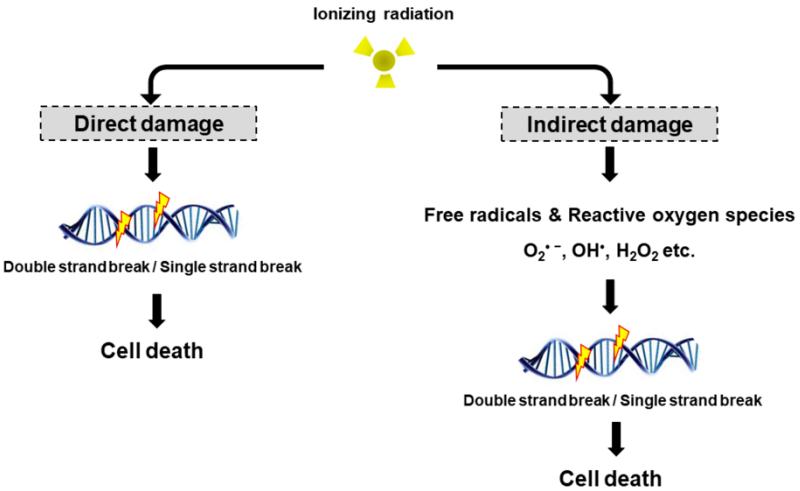

Figure 1. *Direct and indirect gene damage by ionizing radiation. Radiation can directly damage genes. The indirect gene damage is caused by the free radicals derived from the ionization or excitation of the water component of the cells (Hur, 2017).*

However, alpha particles do have limitations. The first problem is their availability, because majority of the alpha radionuclides have half-lives either too short or too long for therapeutic use, their production is not

economically viable or chemical properties do not allow their use in medicine (Majkowska-Pilip, 2020). The short half-life radionuclides that can be used are limited to easily accessible tumors. The less easily accessible sites, where the targeting agent is taken up slowly, or solid tumors where longer penetration time is necessary, need longer-lived alpha emitting particles. The last problem with alpha particles is that the recoiled daughter-nuclides of the long-lived alpha emitting particles can do significant damage to healthy tissues when not retained at the tumor site (de Kruijff, 2015).

A more advanced and selective method for alpha radiotherapy with better outcomes, fewer side effects, and higher efficacy is needed. A promising method is pre-targeted drug delivery with super paramagnetic iron oxide nanoparticles (SPION's). SPION's have great potential due to their biocompatibility, facile synthesis, functionalization and fine-tuning of the properties towards various applications (Revia, 2016).

This paper is part of a bigger project that focuses on the development of functionalized SPION's for pre-targeting of tumor cells for the subsequent in vivo cyclooctyne promoted click-reaction (Ramil, 2013) with an alpha-emitting radionuclide chelated to DOTA-cyclooctyne complex (^{225}Ac-DOTABCN). The principle of this idea is as follows: firstly, the nanoparticles will accumulate at the tumor site, which can be confirmed by magnetic resonance imaging (MRI) due to the convenient magnetic properties of SPIONs. Secondly, an injection of a radiotherapeutic agent will be given which binds to the accumulated nanoparticles on the tumor site via the cyclooctyne click reaction, as shown in Figure 2 (Knight, 2014). As the nanoparticles are not expected to re-enter the bloodstream after accumulation at the tumor site, the effect of the radiotherapeutic agent will only occur locally, resulting in limited damage to healthy tissue surrounding the tumor.

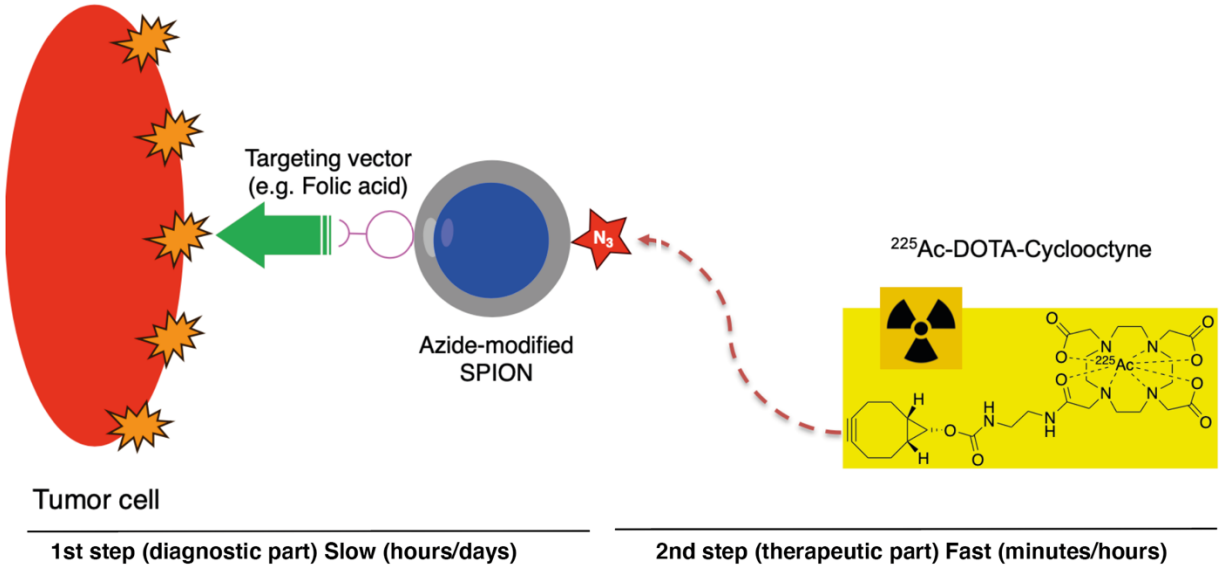

Figure 2. *Schematic representation of the two-step tumor targeting process with cyclooctyne promoted click reaction. Step one shows the first injection with nanoparticles which accumulate at the tumor site, step two is injection of therapeutic agent which while bind to the nanoparticles via the cyclooctyne click reaction.*

SPION's can target tumors passively and actively. Passive targeting happens by the enhanced permeability and retention (EPR) effect. This effect occurs due to the rapid growth of tumors, which requires quick vascularization resulting in abnormal growth of tumor blood vessels. This makes the tumor vascular structure more permeable to macromolecules, like nanoparticles, than that of a normal tissue. The increased permeability and poor lymphatic drainage results in the accumulation of nanoparticles at the tumor site (Stéen, 2018, Zwicke, 2012). Figure 3 shows the passive targeting of nanoparticles by the EPR effect.

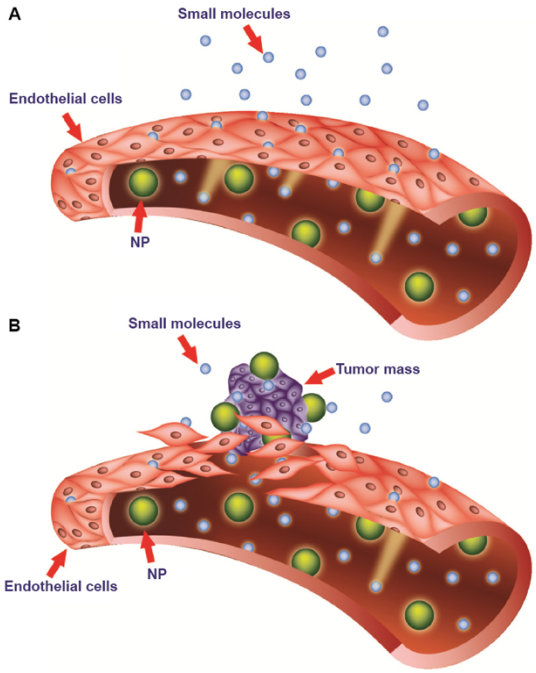

Figure 3 *Difference between normal (A) and tumor (B) blood vessels. Tumor vessels contain larger fenestrations between endothelial cells than normal vessels. This allows nanoparticles (NPs) to reach tumor cells by the enhanced permeability and retention effect (Bozzuto, 2015).*

SPIONs can also be functionalized for active targeting of cancer cells. The nanoparticles are then conjugated with a targeting group that interacts specifically with antigens or receptors that are either uniquely expressed or overexpressed on the cancer cells relative to normal cells (Pearce, 2019). Folic acid (FA) is one of those groups that can actively target tumor cells based on overexpression of folate receptors by the majority of cancer cells compared to healthy tissues (Zwike, 2012).

The behavior of the SPIONs on cancer cells in this report was studied on the glioblastoma multiforme (GBM) cancer cell line U87. U87 cancer cell line was grown in 1966 from the tissue of a 44-year-old woman with an aggressive brain cancer known as GBM (Dolgin, 2016). GBM has a high invasiveness, the propensity to spread through the brain parenchyma and elevated vascularity. This makes these tumors extremely recidivist. Even after surgical procedures and chemoradiotherapy this results in a short survival period for patients (D'Alessio, 2019). GBM has one-year survival rate of 29,6% making it one of the deadliest types of cancer (Clark, 2010).

The U87 cancers cells were grown into spheroids. Spheroids are a three-dimensional in vitro model system that show more resemblance to in vivo tumors than two-dimensional monolayer cell cultures (Khanna, 2020). Spheroids share three characteristics with in vivo tumors: 1) heterogenous cellular growth with proliferating cells at the outside surrounding quiescent cells and a necrotic core; 2) similar pH, nutriments and oxygen gradients; 3) matrix and network of cell-to-cell and cell-to-matrix interactions (Millard, 2017). Figure 4 shows the resemblance of a spheroid and a vivo tumor.

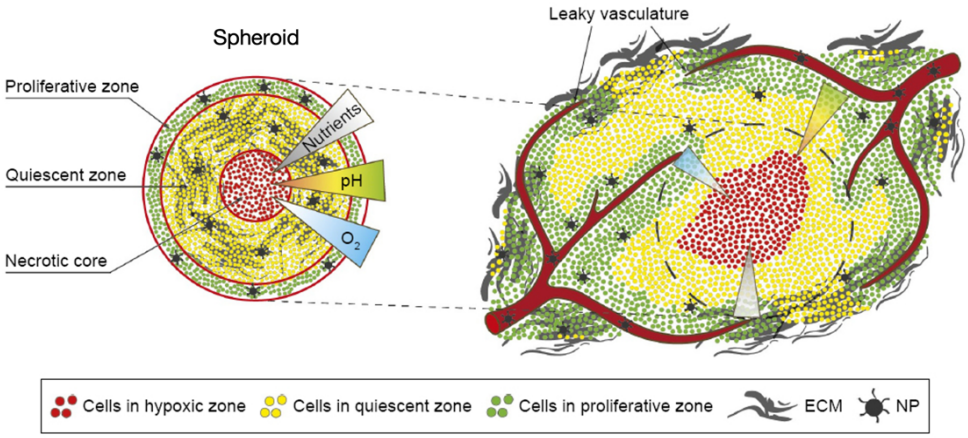

Figure 4. *Schematic representation of similarities between spheroid (left) and tumor (right). Spheroid is composed of proliferative cells on the outside surrounding quiescent cells and a necrotic core. Nutrients pH and oxygen are comparable. Abbreviations: ECM, extra cellular matrix, NP, nanoparticle (Millard, 2017).*

Four SPIONs prepared in earlier experiments were evaluated in this study, two with polyethylene glycol (PEG)(SPIONs-PEG-N3-FA-FITC)(SPIONs-PEG-N3-FA) and two without PEG (SPIONs-FA-N3-FITC)(SPIONs-FA-N3), shown in Figure 5. The nanoparticles were made by the following method. 5 – 10 nm SPION's were coated with oleic acid were synthesized via the thermal decomposition method based on the study of Herranz et al. with some modifications (Herranz et al., 2008). Afterwards, the FA, azide, FITC (fluorescein isothiocyanate) for SPIONs-FA-N3-FITC and SPIONs-PEG-N3-FA-FITC, and PEG for the SPIONs-PEG-N3-FA-FITC and SPIONs-PEG-N3-FA were functionalized to the SPIONs as silane conjugates, this procedure was adapted from the study Bloemen et al. (Bloemen et al., 2012).

All the modifications made to the SPIONs have been done with a specific purpose. The groups that are common for all the SPIONs are FA and azide. FA groups were used for the active targeting of the cancer cells, because cancer cells, including U87 cancer cells, overexpress the FA receptor (Low, 2009). The azide groups were used for two-step targeting strategy based on the bioorthogonal mechanism by using cyclooctyne promoted click reaction between azide and a radiation emitting DOTA complex. The FITC groups were placed on the SPIONs-FA-N3-FITC and SPIONs-PEG-N3-FA-FITC nanoparticles as labels to visualize the nanoparticles by fluorescence microscopy.

The functionalized group where SPIONs-FA-N3-FITC and SPIONs-PEG-N3-FA-FITC, SPIONs-FA-N3 and SPIONs-PEG-N3-FA differ is PEG. PEG is known as a stealth polymer and is widely used in drug delivery

systems (Mohapatra, 2019). PEG functionalization is able to modify the pharmacokinetic and pharmacodynamic properties, and biodistribution of molecules, improving the solubility and stability, prolonging the body-residence time, assuring a sustained drug concentration and decreasing the immunogenicity (Milla, 2012).

The SPIONs-FA-N3 and SPIONs-PEG-N3-FA nanoparticles will be used in combination with the radionuclide Lutetium-177 (^{177}Lu) linked to DOTA-complex (^{177}Lu-DOTA-cyclooctyne) made in earlier experiments. ^{177}Lu decays to stable Hafnium-177 by emission of β^- particles with a maximum energy of 497 keV, which is suitable for treating small- and medium-sized tumors (Banerjee, 2015). This research will treat U87 GBM cancer cells with ^{177}Lu-DOTA-cyclooctyne with dose of 0.1 and 1 MBq. These doses were chosen based on the results of cell viability analyses of another research (Poty, 2020). We used ^{177}Lu-DOTA-cyclooctyne instead of ^{225}Ac-DOTA-cyclooctyne because ^{177}Lu was available. While ^{177}Lu-DOTA-cyclooctyne does not have the same the same effect as ^{225}Ac-DOTA-cyclooctyne it does suffice as a model to study the cyclooctyne promoted click reaction.

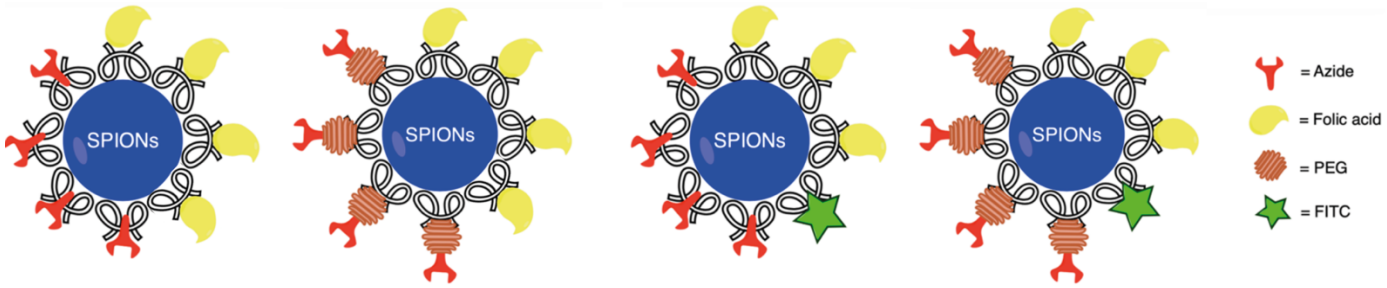

Figure 5. *Schematic representation of SPIONs from left to right SPIONs-N3-FA, SPIONs-PEG-N3-FA, SPIONs-N3-FA-FITC, SPIONs-PEG-N3-FA-FITC. Abbreviations: PEG, polyethylene glycol, FITC, fluorescein isothiocyanate.*

The goal of this research is to observe the behavior of the SPIONs-FA-N3-FITC and SPIONs-PEG-N3-FA-FITC nanoparticles when added to U87 spheroids for 4 and 24 hours and to verify whether the nanoparticles are internalized by the cancer cells or stay on the outside of the membrane. This will be done by growing spheroids of U87 and incubating them with the nanoparticles. After the incubation the spheroids will be cryo cut into slices and analyzed with a fluorescence microscope and with inductively coupled plasma optical emission spectrometry (ICP-OES). ^{177}Lu-DOTA-cyclooctyne with radioactivity of 0.1 and 1 MBq was added to spheroids incubated with SPIONs-FA-N3 and SPIONs-PEG-N3-FA nanoparticles and analyzed with an inverted microscope over a period of 7 days to study the click reaction of the nanoparticles with the ^{177}Lu-DOTA-cyclooctyne.

In this report the following will be discussed. In chapter 2, the Materials and Methods of the experiments performed are described. In chapter 3, the Results and Discussion of the experiments are presented. Chapter 4 contains the Conclusion of the report and finally chapter 5 concerns recommendations on further research of this topic.

2 Materials and Methods

Chemicals

U87 GMB cells were supplied by VU Medical Center, Dulbecco's Modified Eagle Medium (Dmem) High Glucose from biowest, 5% Fetal Bovine Serum (FBS) from biowest, Penicillin-streptomycin solution from biowest, Phosphate buffered saline (PBS) from biowest, Trypsine-EDTA 1x from biowest, MemBrite™ Fix 569/580 Cell surface Staining kit from Biotum, Paraformaldehyde (PFA) 4% supplied by the lab, NucBlue™ fixed cell stain from Thermo Fisher, PELCO Cryo-Embedding Compound transparent freezing medium from Ted Pella, 67% nitric acid from Thermo Fisher, Milli-Q (MQ) water created with a MQ water machine, ^{177}Lu supplied by Erasmus Medical Center.

Instruments

Inverted microscopy was conducted with a SZ 45 B zoom Binocular stereo microscope 7x-45x under the following conditions: 2x magnification, photos were taken with camera and analyzed with samplescan.

Fluorescence microscopy was conducted with a KERN transmitted light microscope OBN-14 under the following conditions: 20x magnification, photos were taken with lens 2, 3 and 4, program to analyze the pictures was Microscopevis2.0pro, ImageJ was used to merge the photos taken with the different lenses.

Inductively coupled plasma – optical emission spectrometry (ICP-OES) was conducted with an OPTIMA 4300DV Perkin Elmer ICP-OES (Perkin Elmer, Waltham, MA USA) under the following operating conditions: RF power 1350 W, nebulizer gas flow 0.8 L/min, auxiliary gas flow 0.2 L/min sample, Sample Flow Rate 1.50 mL/min. The detection wavelengths: 238.204, 239.256, 259.939, 234.349, 234.83, 238.863, 273.955 nm were selected for the quantification of Fe.

Cryosection on the spheroids was performed with a cryostat Leica CM1900. The cryostat was operated under the following conditions: Room of cryostat temperature -25°C, cutting table temperature -20°C, cutting size was set to 14 or 16 µm, freezing medium PELCO Cryo-Embedding Compound was used to freeze the samples.

Methods

Growing and passage of cells

The cells of U87 were passaged once a week. The cancer cells should reach at least about 80-90% of confluency (Souster, 2020), therefore the U87 GBM cells were passaged once a week, in order to keep them healthy and prevent contamination. The medium used for the cell growth and the passages consisted

of 45 mL DMEM, 5 mL serum and 0,5 mL penicillin. The DMEM medium is designed to support the growth of the cancer cells, is composed of amino acids, vitamins, inorganic salts and glucose. However, the medium also needed an addition of serum as a source of hormones, as well as growth- and attachment factors. The medium helps to maintain pH and osmolality. The antibiotics penicillin-streptomycin were added to control the growth of bacterial and fungal contaminants. (Arora, 2013) The old medium was pipetted out of the flask and the flask with the cancer cells was washed twice with 2 mL PBS. PBS is a balanced salt solution that provides an environment that helps to maintain the structural and physiological integrity of cells in vitro (Thermo Fischer 1, 2021). 1 mL trypsin was added to the flask and kept for 6 min in a 37°C incubator to release the cells from the bottom. After 6 min, the flask was taken out of the incubator and checked under a microscope to see if the cells were detached from the bottom and from each other, if the cells were still stuck then the flask was gently tapped on the counter. The cancer cells are only incubated for 6 min with trypsin to prevent the trypsin from cleaving of the cell surface growth factor receptors or membrane proteins (Huang, 2010). 2 mL of medium was added to the trypsin and the solution was centrifuged for 5 min at 2000 rpm. The 3 mL solution of medium and trypsin was pipetted out leaving the cells behind, 1 mL of medium was added to the cells and mixed by pipetting the solution in and out a couple of times. 20 µL is of this solution was pipetted in the cell counter disk. The cells were counted with a LUNA II cell counter and a certain amount of the cell suspension was brought into the new flask depending on the amount cells. This flask was kept at 37°C in the incubator until next passage or other use.

Growing U87 spheroids in 96 u-shape well plate

Spheroids were grown by seeding of a 96 well U-round bottom plate, which was done during the cells passage. 96 well U-round bottom plate was used because the well shape promotes the formation of a single spheroid (Bresciani, 2019). After counting the cells, a dilution with medium was prepared, depending on the number of cells counted with a LUNA II cell counter. The suspension used for this work was 10^4 cells/mL. 200 µL of this suspension was added to the separate wells in the 96 well plate. All the wells on the outside of the 96 well plate were filled with 200 µL PBS. The 96 well plate was then incubated for certain number of days, depending on the desired size of the spheroids in the incubator at 37°C.

Nanoparticles

The nanoparticles SPIONs-FA-N3-FITC and SPIONs-PEG-N3-FA-FITC, needed to be diluted to 100 µg/mL before they were added to the spheroid. This was done by first adding 1 mL PBS to 1 mg of nanoparticles. The solution was then sonicated until the nanoparticles were fully dispersed in the PBS. Finally, 9 mL of medium was added and the solution was irradiated with UV-light for 5 min to prevent bacterial contamination of the spheroids. Then, the 150 µL nanoparticles solution was added to the spheroids in the 96 well plate after first pipetting 150 µL of old medium out of the wells. This was done 4 and 24 hours before staining and fixating the spheroids.

Staining spheroids

To stain membranes of the spheroids, 150 µL of medium was taken out of the wells of the 96 well plates and rinsed 3 times with 150 µL PBS. Prestaining solution was made by diluting 1 µL pre-stain with 1 mL PBS. 150 µL PBS out was taken out of the wells that were going to be treated with dye and 150 µL of prestaining solution was added and kept in the incubator at 37°C for 5 min. The staining solution was made by diluting 1 µL pre-stain with 1 mL PBS. 150 µL prestaining solution was taken out and 150 µL of staining solution was added. 96 well plate with staining solution was then kept for 5 min in the incubator at 37°C. After 5 min, the staining solution was taken out and washed 3 times with 150 µL PBS. Then all the wells were washed 3 times with PBS. 150 µL PBS was taken out from all the wells and 150 µL of 4% PFA was added to fixate the spheroids. The 96 well plate was incubated for 15 min in room temperature. Finally, 150 µL 4% PFA was taken out and the spheroids were washed 3 times with 150 µL PBS. Fixation is needed to make a snapshot of a cell state. Without fixation, the structures in cells would fall apart and diffuse away. PFA causes covalent cross-links between molecules, effectively gluing them together. (Hobro, 2017). The spheroids could then be stored in PBS in the fridge.

Cryo-section

The stained spheroid was pipetted in the tip of 2 mL Eppendorf vial and all the PBS was pipetted out while keeping the spheroid in the tip. Transparent tissue freezing medium was added until the tip was filled, making sure the spheroid stayed in the tip. The tip of the vial was then placed in the chamber of the cryostat, where it was frozen. Transparent tissue freezing medium was added on to a cooled cutting table. When the medium in the tip was frozen it could be taken out of the tip and added to the medium on the cutting table. Medium was added to the cutting table to glue frozen medium from the tip and the frozen medium on the cutting table to each other. It is important to see where the spheroid was in the medium, to know when the spheroid will be cut. The cutting table was set back in the cryostat to let it freeze. The cutting of the medium could start once it was completely frozen. The cryostat cutting size was set to 14 or 16 µm and the temperature of the room of the cryostat was set to -25°C, the temperature of the holder of the cutting table was set to -20°C. The first slices that were cut did not yet contain the spheroid. The first cut slices were checked regularly under the microscope to see if the spheroid is being cut. The spheroid could not always be seen by the eye, especially not in the first slices of the spheroid. The slices that did contain the spheroid were collected on 16x16mm coverslips and numbered. Slices were made until the spheroid could not be seen under the microscope. The last slide functioned as zero point from where the spheroid starts and how deep the other slices were in the spheroid.

Fluorescence microscopy

The slices made with the cryostat were not covered to preserve them for the microscope images to prevent crushing or breakage of slices by a cover slip. The fluorescence microscope was turned on 15 min before use. DAPI was added to the slice just before using the microscope. Before the pictures can be taken the slice of the spheroid has to be sought and then the microscope must be focused. 3 pictures were taken of

every slice with 3 filters, each set to 635, 543 and 488 nm. After the images were taken, the slices were covered with another microscope glass and glued together with nail polish. The covered slices were then stored in the fridge until used for the ICP. The 3 images of the slices were merged in ImageJ.

ICP-OES

Calibration curve was made by measuring Fe solutions of 1, 2, 3, 4 and 5 mg/L. With this calibration served to determine the iron concentration in the cryosection slices as the result of accumulation of nanoparticles.

ICP analysis was done on the slices made from the cryosection. The slices from the cryosection were dissolved from the microscope slices by putting them in a 50 mL tube, adding 1 mL of 67% nitric acid and letting it sit overnight. The solution of slices in nitric acid were diluted the next day with 9 mL MQ water, 5 mL of this solution was then transferred to a 15 mL tube, which could then be used for the ICP-analysis.

177Lu-DOTA-cyclooctyne experiment

Method “Growing and passage of cells” was used to supply the U87 cancer cells and method “Growing U87 spheroids in 96 U-shape well plate” was used for growing the U87 spheroids. Nanoparticles SPIONs-FA-N3 and SPIONs-PEG-N3-FA were prepared with method “Nanoparticles” and added 4 hours before adding ^{177}Lu-DOTA-cyclooctyne. ^{177}Lu-DOTA-cyclooctyne was diluted to 1MBq and 0.1MBq. 1MBq ^{177}Lu-DOTA-cyclooctyne solution was made by diluting 186 µL 12.1 MBq with 165 µL PBS and 1 mL medium. 0.1 MBq ^{177}Lu-DOTA-cyclooctyne solution was made by diluting 18.6 µL 12,1 MBq with 16.5 µL PBS and 1.315 mL medium. The ^{177}Lu-DOTA-cyclooctyne solution was added to the wells by first pipetting 150 µL of medium out of the wells and adding 150 µL of ^{177}Lu-DOTA-cyclooctyne solution. The 96-well plate was then incubated for 30 min. After the incubation, 150 µL of ^{177}Lu-DOTA-cyclooctyne was taken out and the spheroids were washed with 150 µL of PBS 3 times. Finally, 150 µL of medium was added to the washed spheroids and the 96-well plate was incubated for 7 days. The medium in all the wells was refreshed on day 4 and day 6 after the ^{177}Lu-DOTA-cyclooctyne treatment. Pictures with inverted microscope at 2x magnification were taken 0, 1, 4, 5, 6, and 7 days after treating the spheroids with ^{177}Lu-DOTA-cyclooctyne. The spheroids were fixed 7 days after addition of the ^{177}Lu-DOTA-cyclooctyne by washing them 3 times with 150 µL PBs, incubating them with 150 µL 4% PFA for 15 minutes for fixation and washing them 3 times with 150 µL PBS again. The spheroids were stored in PBS in the fridge.

3 Results and Discussion

Cryosection

To verify how the nanoparticles SPIONs-FA-N3-FITC and SPIONs-PEG-N3-FA-FITC behave on a U87 GMB spheroid, it was chosen to incubate the spheroids for 4 and 24 hours. Earlier experiments showed that 2 hours incubation did not show enough attachment of the nanoparticles to the spheroids. After the incubation, the spheroids were cut into slices of 14-16 µm, which corresponds approximately to one layer of U87 GMB cells (Bionumbers, 2021). The cryo section was done in triplicate for each set of nanoparticles at different incubation times. Appendix A shows the best performed cryo section of these spheroids. Cryosection technique was used because it allows to observe the interior U87 spheroids with multiple slices. In this way, it was possible to see how deep the nanoparticles penetrate the spheroid.

Size of the spheroids cryosection

The spheroids used for the cryosection, were grown for 6 days before adding the nanoparticles and had an average diameter of 438 µm, as determined from the inverted microscope images. The spheroids were grown to this size because spheroids of 300–500 µm of size are those that best mimic in vivo tumors in terms of hypoxia and proliferation gradients (Pinto, 2020). When cutting the spheroid, it was unclear when the cutting of the spheroid started, but it was clear when no spheroid was being cut. Knowing when the spheroid was stopped being cut it is possible to count back the slices to determine approximately how deep the slices are in the spheroid, because the size of the spheroid is known. Figure 7 shows a 3D visualization of a spheroid and the depth in µm. The size of the slices and the depth of the nanoparticles in the slices are harder to determine because the slices transform after being cut and when they are transferred from the cryo cutter on to microscope slices. The spheroids had an average size of 438 µm and the cryo-section was set to make 14 – 16 µm thick slices of the spheroids. This means that a maximum of 27 – 31 slices could be made of the spheroids if the cryo-section went perfect. This was not always the case, as the average number of slices per spheroid in the cryo-section was 15 – 20.

Orientation spheroid in freezing medium cryosection

The nanoparticles tend to primarily cluster on one location on the spheroid, which could be seen with the naked eye before the cryosection, as also shown in the cryosection results. The place where the nanoparticles cluster is different for every spheroid because the spheroids cannot be cut the same way every time. The orientation of the spheroid in the freezing medium, and therefore, the position of the cluster of nanoparticles differs for every cryosection of a spheroid. This should be kept in mind when drawing conclusions from the cryosection results. Figure 8 shows how the orientation of the spheroid influences the pictures of the slices.

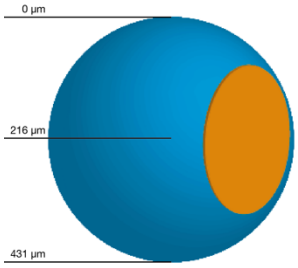

Figure 7. *3D visualization of the depth of slices in the spheroid. Blue is the spheroid, orange cluster of nanoparticles.*

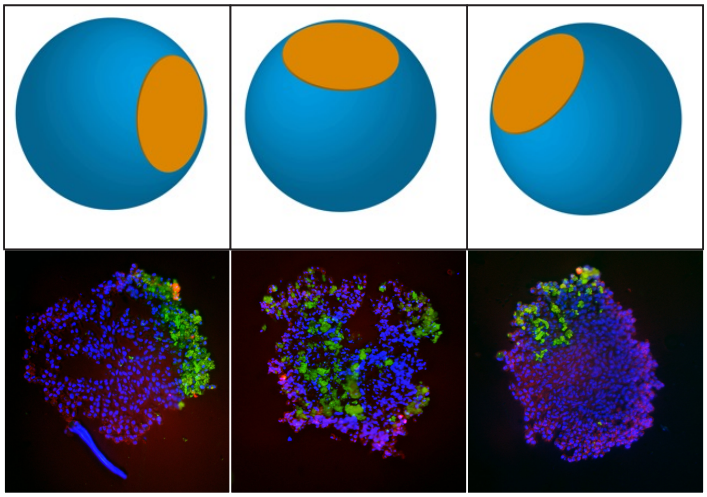

Figure 8. *Influences of orientation of spheroid in freezing medium on pictures of slices. Blue is the spheroid, orange cluster of nanoparticles.*

Results Fluorescence Microscopy cryosection

The slices of the spheroids were analyzed with a fluorescence microscope using three different filters. Three images taken on every slice were merged with ImageJ. The first filter set to emission between wavelength 610 to 750 nm showed the Membrite-stained cell membrane as a red color. The second filter with emission between wavelength 500 to 570 nm showed the FITC group on the nanoparticles with as green color. Finally, the third filter with emission between wavelength 450 to 500 nm showed the DAPI-stained nucleus of the cells as a blue color. Figure 9 shows the emission spectra of Membrite, FITC and DAPI. Figure 10 shows the 3 different pictures and the merged picture of one slice.

It can be seen in figure 10A that the red membrane dye is not visible in the whole slice of the spheroid. The red color gradually decreases toward the center of the spheroids, which is likely explained by the diffusion gradient. The dye stains the cells at the periphery of the spheroid more than at the cells within the core of the spheroid (Tchoryk, 2019).

The nanoparticles can interact in a couple ways when brought in contact with a U87 spheroid: 1) agglomerate with other nanoparticles without being attached to the spheroid; 2) attach to the cancer cells at the outer layer of the spheroid; 3) diffuse into the spheroid between the cancer cells; 4) penetrate the cancer cells. The fluorescence microscope can only show where the nanoparticles are in the slice of the spheroid, but possible internalization of nanoparticles by the cells can unfortunately not be distinguished.

The functional groups conjugated to the surface of nanoparticles are expected to influence their interacting behavior with the cancer cells. FA is present on both nanoparticles and actively targets the cancer cells. Based on overexpression of folate receptors, the FA groups present on both nanoparticles are expected to increase their affinity towards U87 GBM cancer cells (Zwike, 2012).

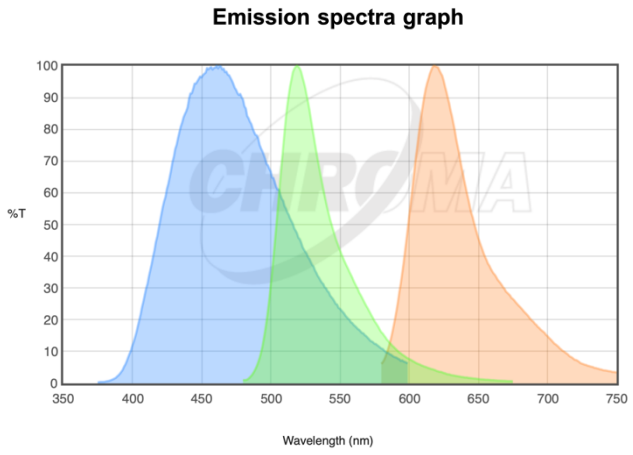

Figure 9. *Emission spectra of Membrite (orange), FITC (green) and DAPI (blue)*

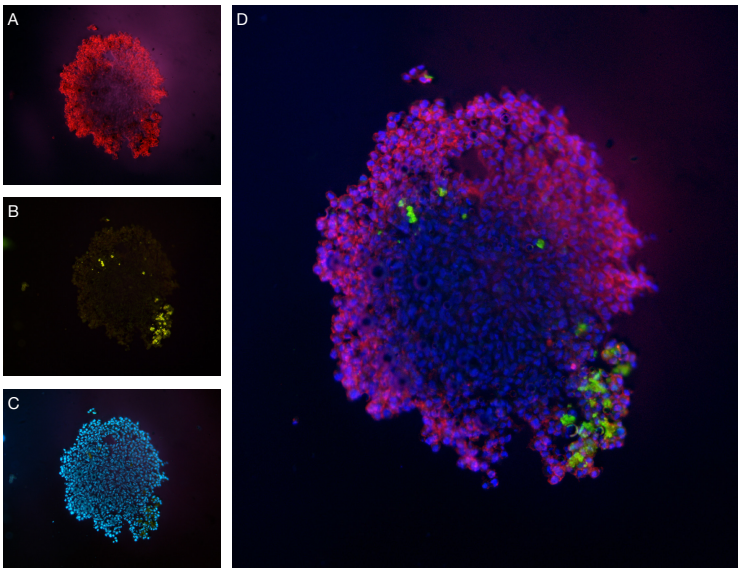

Figure 10. *Photos taken with fluorescence microscope. A: Membrit-stained cell membrane in red, B: the FITC groups on the nanoparticles in green, C: the cell nucleus stained with DAPI in blue and D: merged images of A, B and C.*

The presence of PEG (nanoparticles SPIONs-PEG-N3-FA-FITC) is expected to reduce the cellular uptake of SPIONs (Dulińska-Litewka, 2019, Lassenberger, 2017). Uncoated SPIONs have a positive charge at the surface which can interact with the negatively charged interface of the cell membranes. However, when PEG is added to the SPIONs it can be sufficient to screen this interaction (Gal, 2017). Therefore, it is expected that the uptake and diffusion of nanoparticles into the spheroid will be higher for the SPIONs-FA-N3-FITC nanoparticles than for the SPIONs-PEG-N3-FA-FITC nanoparticles.

Cryosection Results

The fluorescence microscope photos of the cryosection of the spheroids treated with SPIONs-FA-N3-FITC for 4 hours can be seen in figure 11 in column A. The images show that some amount of nanoparticle is attached clustered on one side of the spheroid and inside the spheroid. Small amounts of nanoparticle can be seen on other places in the spheroid but not further moved into the spheroid than the clustered nanoparticles. The 24 hours incubation can be seen in figure 11 in column B. Significant number of nanoparticles is moved into the spheroid after 24 hours incubation. The nanoparticles are still clustered on one side, but diffusion reaches the middle of the spheroid. There was no membrane dye used in this cryosection, the cryosection of this nanoparticle and incubation time in the appendix A does have membrane dye. This cryosection was chosen here because it showed the best comparison with the other cryosections.

Figure 11 column C shows the cryosection of the spheroids treated with SPIONs-PEG-N3-FA-FITC for 4 hours. The nanoparticle shows resemblances to the spheroids treated with SPIONs-FA-N3-FITC nanoparticle for 4 hours. Small number of nanoparticles is clustered on the outside of the spheroid, the nanoparticles hardly moved further into the spheroids. Column D of figure 11 shows the cryosection of the

24 hours incubation time. The nanoparticles are clustered on one side and moved further into the spheroid than the nanoparticles that were incubated for 4 hours. However, the dept that the SPIONs-PEG-N3-FA-FITC particles go into the spheroid is significantly less than that of the of the SPIONs-FA-N3-FITC nanoparticles, this probably is caused by the PEG group on the SPIONs-PEG-N3-FA-FITC nanoparticle.

The results of the cryosection are in line with the expectations based on literature. The SPIONs-PEG-N3-FA-FITC nanoparticles move less far into the spheroid than the SPIONs-FA-N3-FITC nanoparticle. The uptake of SPIONs-FA-N3-FITC nanoparticles seems higher than the uptake of the SPIONs-PEG-N3-FA-FITC nanoparticles. An ICP-OES analyses of whole spheroids incubated with the nanoparticles and of the cryosection slices were done to confirm this. The results of the ICP analyses are discussed in section “ICP-OES”.

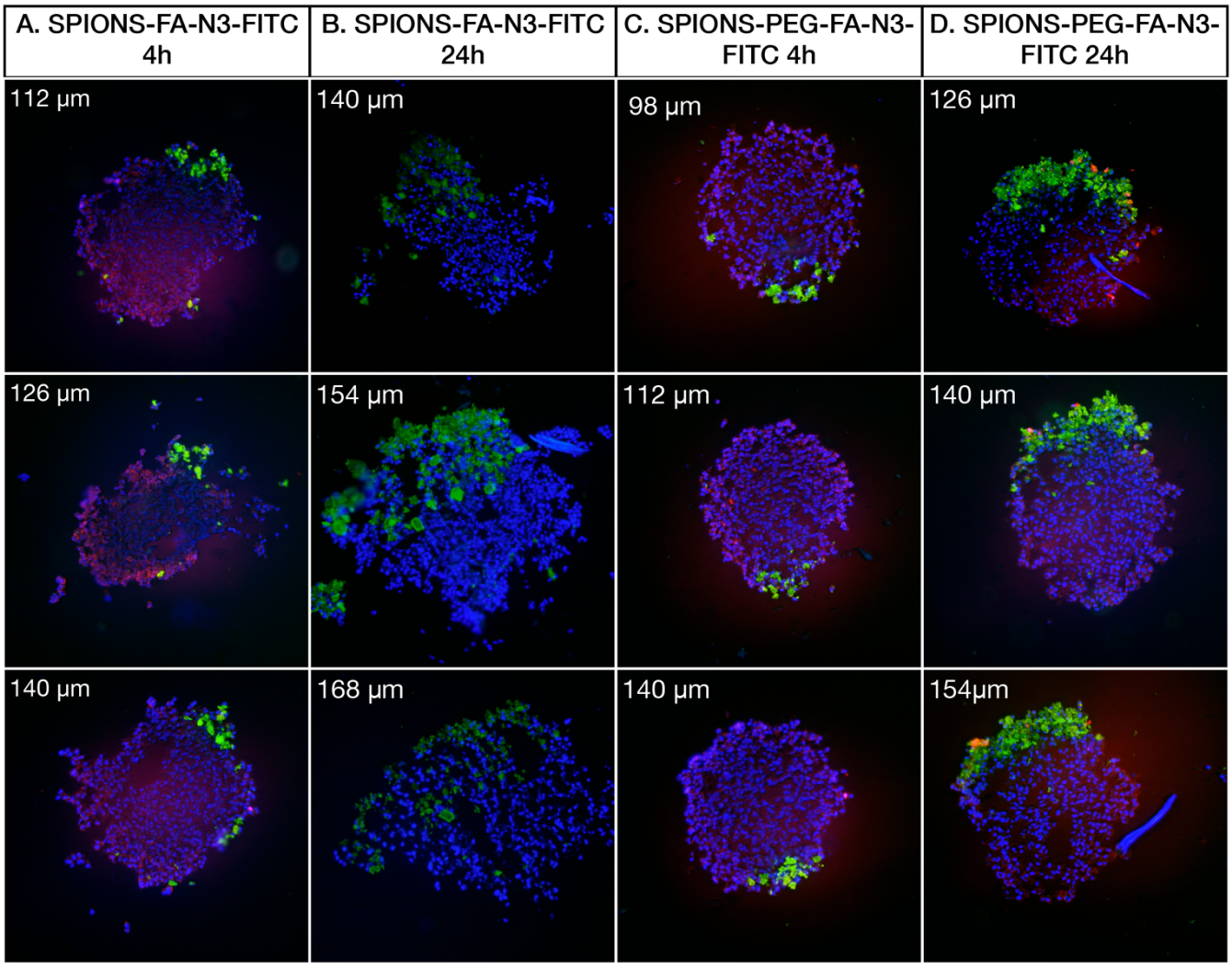

Figure 11. *Fluorescence microscopic images on cryosections of spheroids incubated with SPIONs-FA-N3-FITC and SPIONs-PEG-N3-FA-FITC nanoparticles for 4 hours (column A - SPIONs-FA-N3-FITC and column C - SPIONs-PEG-N3-FA-FITC) and 24 hours (column B - SPIONs-FA-N3-FITC and column D - SPIONs-PEG-N3-FA-FITC). The size of the spheroids is around 435 µm, the depth of the slice is indicated in the left upper corner of each image.*

ICP-OES

ICP-OES analysis was used to determine the concentration of iron in the cryosections in order to estimate the number of nanoparticles retained by the spheroids after incubation with differently functionalized SPIONs. The spheroids treated with SPIONs-FA-N3-FITC and SPIONs-PEG-N3-FA-FITC for 4 and 24 hours with the most successful cryosections were chosen for analysis with ICP-OES.

Next to the slices of the cryosections, the whole spheroid incubated with 150 µL of SPIONs-FA-N3-FITC nanoparticles (4 and 24 hours), SPIONs-PEG-N3-FA-FITC nanoparticles (4 and 24 hours), were analyzed by ICP-OES (Table 1).

Sample	Concentration Fe in mg/L
SPIONs-PEG-N3-FA-FITC 24h spheroid	3,00E-02
SPIONs-PEG-N3-FA-FITC 4h spheroid	7,74E-03
SPIONs-FA-N3-FITC 24h spheroid	3,36E-02
SPIONs-FA-N3-FITC 4h spheroid	5,17E-03
Black marker	2,00E-04
150 microliter SPIONs-PEG-N3-FA-FITC	2,53E-01
150 microliter SPIONs-FA-N3-FITC	1,92E-01
Freezing medium	2,75E-04

Table 1. *ICP-OES analysis of the whole spheroids treated with nanoparticles SPIONs-FA-N3-FITC and SPIONs-PEG-N3-FA-FITC for 4 and 24 hours, the black marker used to label the slices, the nanoparticles incubation solutions and the freezing medium used for the cryosection.*

The uptake of the SPIONs-PEG-N3-FA-FITC and SPIONs-FA-N3-FITC nanoparticles can be determined by dividing the uptake of the 4- and 24-hour incubation spheroids by the total of nanoparticles, 150 µL SPIONs-PEG-N3-FA-FITC and SPIONs-FA-N3-FITC. The uptake of SPIONs-PEG-N3-FA-FITC nanoparticles for 4 hours is 3% and for 24 hours is 12%. The uptake of SPIONs-FA-N3-FITC nanoparticles for 4 hours is 3% and for 24 hours is 18%. This is in accordance with results of the fluorescence microscopy images, which showed that after 24 hours more nanoparticles were inside the spheroid compared to 4 hours. The difference between the SPIONs-FA-N3-FITC and SPIONs-PEG-N3-FA-FITC at 24-hour incubation could be caused by the PEG group on the SPIONs-PEG-N3-FA-FITC nanoparticles, which is in compliance with literature (Dulińska-Litewka, 2019, Lassenberger, 2017, Gal, 2017).

Table 1 also shows the ICP-OES results of the black marker used to label the slices and the freezing medium, it shows that these contain Fe and that this can influence the Fe concentration of the cryosection slices. Therefore, the concentration of the freezing medium and the marker are subtracted of the concentration of the cryosection slices. When adding all the Fe concentrations of the slices of one single cryosection, it is expected that this Fe concentration would match the Fe concentration of the whole spheroid treated with the same nanoparticle for the same amount of time. Though the sum of the concentrations of the slices of the cryosection for all 4 spheroids have a higher value than the 4 whole

spheroids treated with the same nanoparticle for the same amount of time. Further research is needed to find out what is causing higher Fe concentration.

The ICP results of the cryosection slices are shown in Figures 14, 15, 16 and 17. It appears that there are traces of Fe in the slices, which can be due to the presence of nanoparticles or another substance which contains Fe. The higher concentration of iron measured with ICP-OES does not always correspond with the intensities found in fluorescence images (Appendix A). A possible explanation could be that not all nanoparticles found in the slices happened to contain FITC. In Figures 14 and 15, the results of the ICP analysis of the whole spheroid are also displayed for comparison.

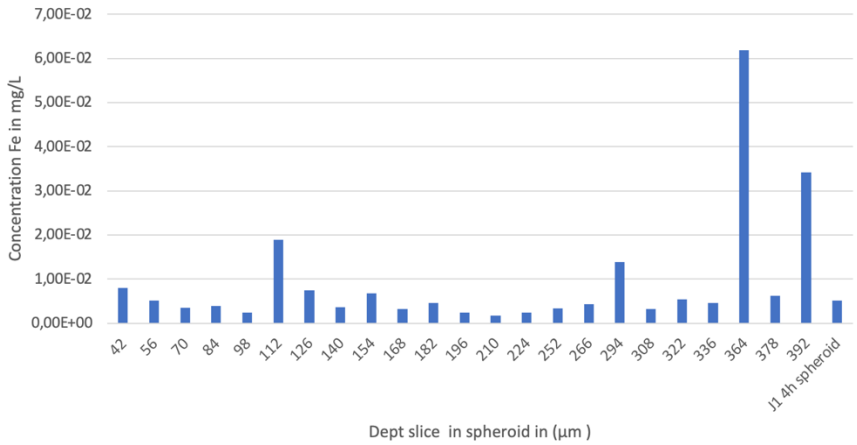

Figure 14. *ICP-OES analysis of the cryosection slices of the spheroid incubated with nanoparticle SPIONs-FA-N3-FITC for 4 hours compared to the ICP-OES analysis of whole spheroid (J1) incubated with nanoparticle SPIONs-FA-N3-FITC for 4 hours.*

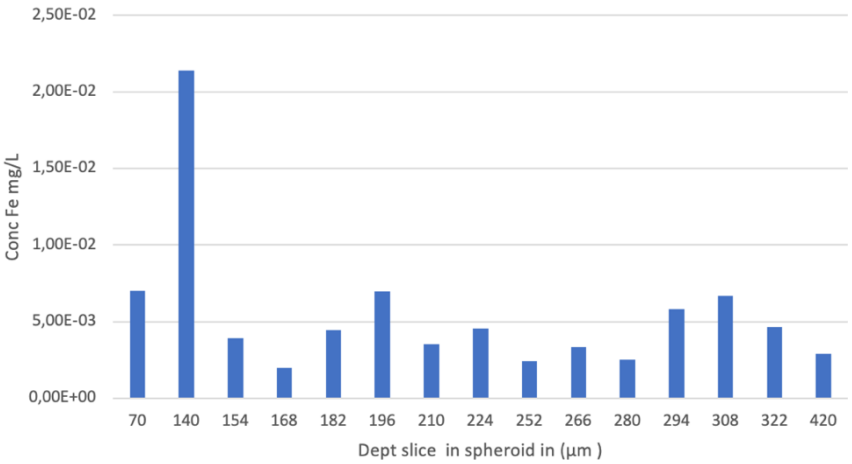

Figure 15. *ICP-OES analysis of the cryosection slices of the spheroid incubated with nanoparticle SPIONs-FA-N3-FITC for 24 hours.*

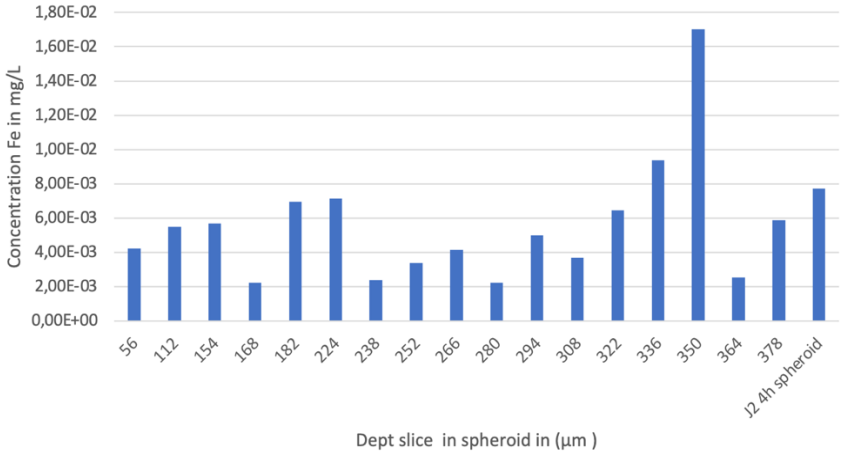

Figure 16. *ICP-OES analysis of the cryosection slices of the spheroid incubated with nanoparticle SPIONs-PEG-N3-FA-FITC for 4 hours compared to the ICP-OES analysis of whole spheroid (J2) incubated with nanoparticle SPIONs-PEG-N3-FA-FITC for 4 hours.*

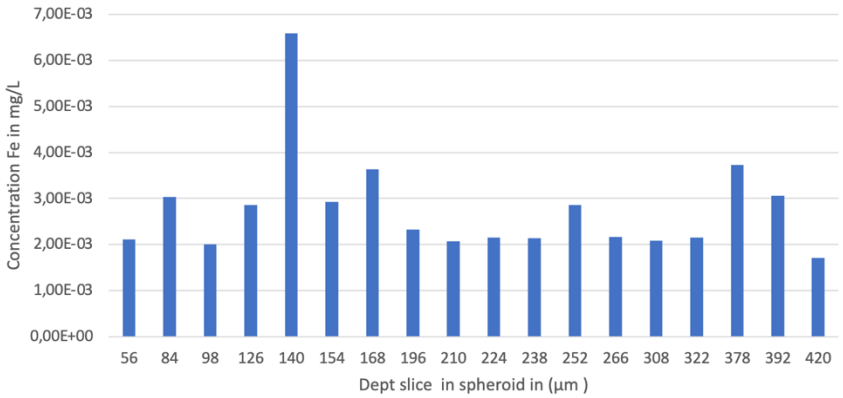

Figure 17. *ICP-OES analysis of cryosection slices of the spheroid incubated with nanoparticle SPIONs-PEG-N3-FA-FITC for 24 hours.*

^{177}Lu experiment

^{177}Lu-DOTA-cyclooctyne complexes with radioactivity of 0.1 and 1 MBq were added to spheroids incubated with SPIONs-FA-N3 and SPIONs-PEG-N3-FA nanoparticles to investigate the effect of the click-reaction with the azide-functionalized nanoparticles retained by the spheroids.

The spheroids were grown for 7 days had an average size of 420 µm before incubation with nanoparticles SPIONs-FA-N3 and SPIONs-PEG-N3-FA and followed by addition of ^{177}Lu-DOTA-cyclooctyne complexes at two different doses (0,1 and 1MBq). The spheroids were treated in 9 different ways, see Table 2.

Spheroid treated with SPIONs-FA-N3	**Spheroids treated with SPIONs-PEG-N3-FA**	**Control spheroids**
Only treated with SPIONs	Only treated with SPIONs	Control
1 MBq ^{177}Lu-DOTA-cyclooctyne	1 MBq ^{177}Lu-DOTA-cyclooctyne	1 MBq ^{177}Lu-DOTA-cyclooctyne
0.1 MBq ^{177}Lu-DOTA-cyclooctyne	0.1 MBq ^{177}Lu-DOTA-cyclooctyne	0.1 MBq ^{177}Lu-DOTA-cyclooctyne

Table 2. *9 different ways the spheroids were treated for the ^{177}Lu experiment*

All the spheroids that were incubated with nanoparticles were washed after the 4 hours incubation and all the spheroids that were treated with ^{177}Lu-DOTA-cyclooctyne for 30 min were also washed. Fresh medium was added and the spheroids were incubated for 7 days. Pictures of all the spheroids were taken with an inverted microscope to monitor the growth on day 0, 1, 4, 5, 6 and 7. The medium of all the wells where the spheroids grew in was refreshed on day 4 and 6 after the Lu-177 treatment, this was done to extend the growth of spheroids (Thermo Fischer 2, 2021). The results are discussed in "*Results ^{177}Lu experiment*".

The spheroids treated with nanoparticle SPIONs-FA-N3 and SPIONs-PEG-N3-FA were incubated for 4 hours, because the cryosection showed that this is enough time for the nanoparticle to attach to the outside of the spheroid. Here the nanoparticles can interact via the azide click reaction with the ^{177}Lu-DOTA-cyclooctyne, the 24 hours incubation showed that more nanoparticles were located inside the spheroid where they are less likely to interact with the ^{177}Lu-DOTA-cyclooctyne via the click reaction.

It is expected that the nanoparticles that are retained on the spheroid after washing will have the click reaction with ^{177}Lu-DOTA-cyclooctyne. The radionuclide can then enter the cell and create cell damage with its radiation, we should observe less growth or shrinkage of the spheroids. Spheroids that are not treated with nanoparticles and only with ^{177}Lu-DOTA-cyclooctyne should show less damage because there is no click reaction. The spheroids treated with 1MBq should show more damage than the spheroids treated with 0.1 MBq, because of the higher dose (Poty, 2017).

Results ^{177}Lu experiment

After incubation of spheroids with nanoparticle and the subsequent addition of radioactive complex, the growth, shape and size were monitored over 7 days. As it can be seen in Figure 12, the spheroids treated with only nanoparticles show resemblance to the control spheroids. This can also be seen in Figure 13, where the mean sizes of the differently treated spheroids are shown. It can also be concluded that the spheroids treated with 0.1 MBq ^{177}Lu-DOTA-cyclooctyne, with and without SPIONs-FA-N3 and SPIONs-PEG-N3-FA nanoparticles do not affect the growth of the spheroid. It is possible that the click reaction and passive retention of has ^{177}Lu-DOTA-cyclooctyne occurred, but that the dose of 0.1 MBq was too low to influence the growth of the spheroids. From the microscope photos it cannot be concluded if the click reaction happened.

The spheroids treated with 1 MBq ^{177}Lu-DOTA-cyclooctyne are affected. The spheroids show cell death and shrinking of size diameter over 7 days. The spheroids that were first incubated with nanoparticles SPIONs-FA-N3 and SPIONs-PEG-N3-FA appear to have more size shrinking and a bigger layer of dead cells around the spheroid one day after the ^{177}Lu-DOTA-cyclooctyne treatment, this can be seen in figure 12, 13 and 14. This implies that the click reaction could have taken place. Figure 14 shows the spheroids treated with 1MBq ^{177}Lu-DOTA-cyclooctyne one day after the treatment, it can be seen that the spheroids treated SPIONs-PEG-N3-FA are more damaged than the spheroids treated with SPIONs-FA-N3. After day 4 the size of the spheroids and the layer of dead cells around the spheroids treated with 1MBq are similar. The spheroids not treated with nanoparticles and only ^{177}Lu-DOTA-cyclooctyne appear to be just as affected. This could be due to the passive retention of the ^{177}Lu-DOTA-cyclooctyne into the spheroids, which can happen without the nanoparticles, but the spheroids were only incubated with ^{177}Lu-DOTA-cyclooctyne for 30 minutes. Other explanation could be that the radiation of the ^{177}Lu-DOTA-cyclooctyne was toxic enough that it effected the spheroids in 30 minutes of exposure.

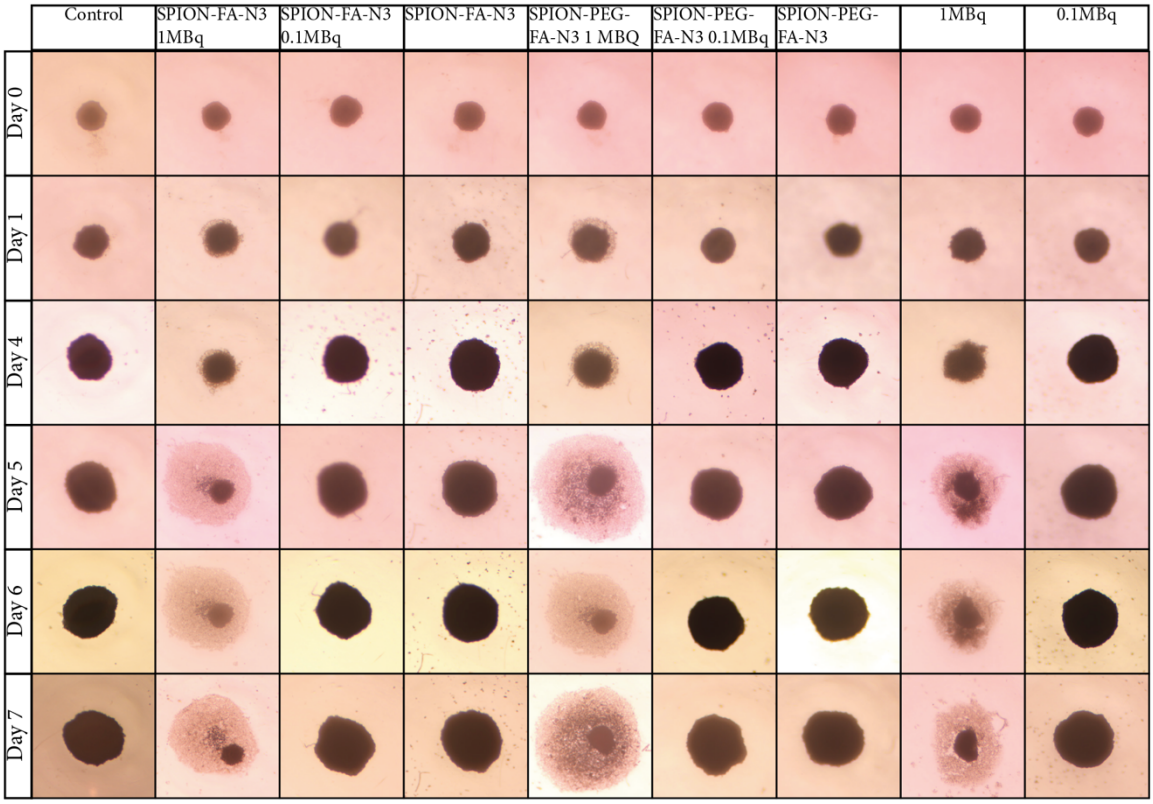

Figure 12. *Inverted microscope images of the spheroids used in the Lu experiment taken over 7 days. From left to right columns: control spheroid, spheroid treated with SPIONs-FA-N3 nanoparticles and 1MBq Lu-177, spheroid treated with SPIONs-FA-N3 nanoparticles and 0.1 MBq Lu-177, spheroid treated with SPIONs-FA-N3 nanoparticles, spheroid treated with SPIONs-PEG-FA-N3 nanoparticles and 1 MBq Lu-177, spheroid treated with SPIONs-PEG-FA-N3 nanoparticles and 0.1MBq Lu-177, spheroid treated with SPIONs-PEG-FA-N3 nanoparticles, spheroid treated with 1 MBq Lu-177 and spheroid treated with 0.1 MBq Lu-177.*

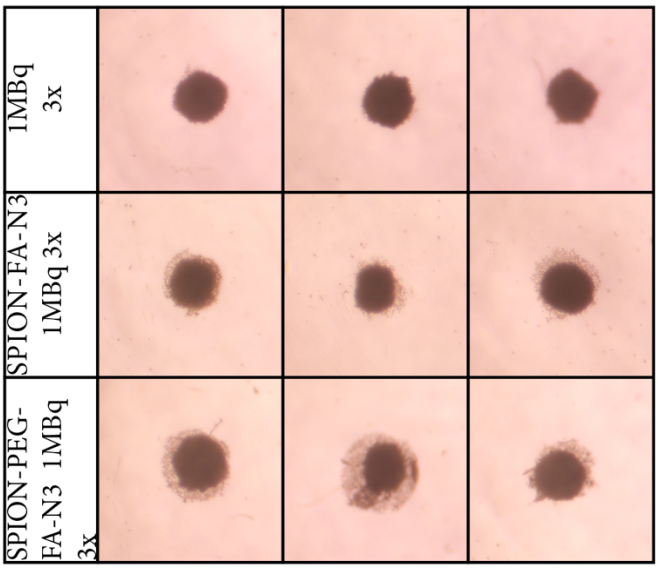

Figure 13. *Inverted microscope images of a spheroids treated with 1MBq ^{177}Lu-DOTA-cyclooctyne one day after treatment. First row shows the 3 spheroids only treated with 1MBq ^{177}Lu-DOTA-cyclooctyne, second row shows the 3 spheroids that were incubated with SPIONs-FA-N3 and treated with 1MBq ^{177}Lu-DOTA-cyclooctyne, the third row shows the 3 spheroids that were incubated with SPIONs-FA-N3 and treated with 1MBq ^{177}Lu-DOTA-cyclooctyne.*

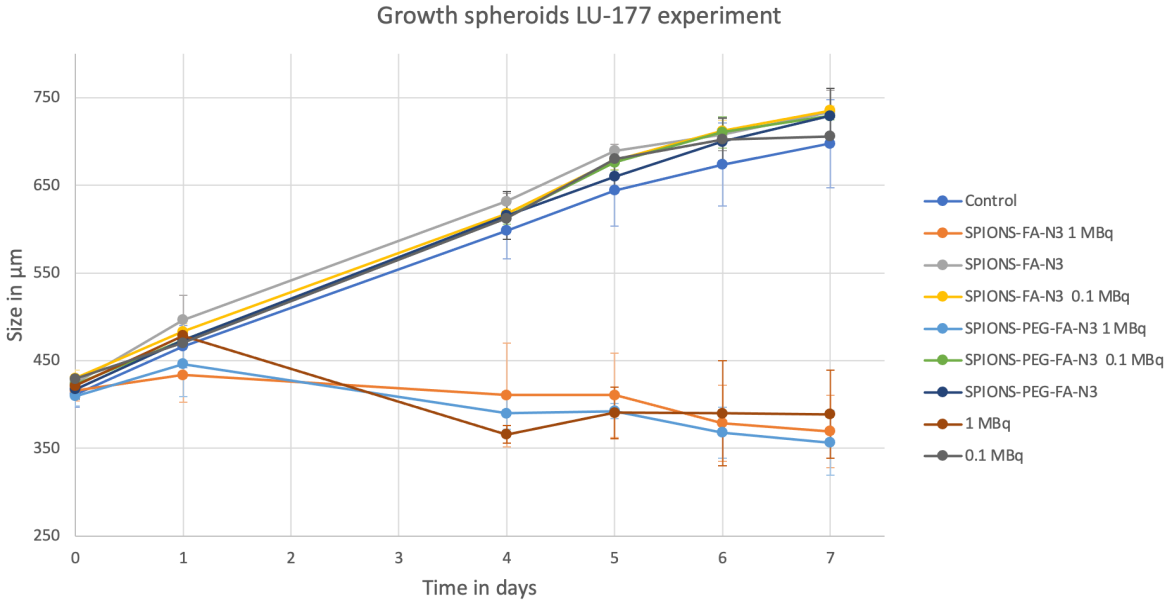

Figure 14. *Growth of the diameter of the spheroids. This graph shows the growth curve of the diameter of the spheroids over 7 days after the 177Lu-DOTA-cyclooctyne treatment. The legend on the right indicates which color portraits the growth curve of the spheroid with the specific treatment. The error bar indicates the results of the triplet experiment that was done for every treatment.*

The spheroids that were treated with 1 MBq ^{177}Lu-DOTA-cyclooctyne had a layer of dead cells around them that loosened when the medium got refreshed. The size of the spheroids shown in Figure 14 on day 4 and 6 is the size of the spheroid after the medium is refreshed. Figure 15 shows the growth of the spheroids treated with ^{177}Lu-DOTA-cyclooctyne over 7 days and the influence of the handling of the spheroids with the pictures before and after the spheroid is treated with something.

Figure 15 also shows images of the spheroids that were just treated with nanoparticles and after 4-hour incubation. The spheroids were washed with PBS after the incubation with the nanoparticles and after the incubation with ^{177}Lu-DOTA-cyclooctyne. All the nanoparticles and DOTA-complexes that were not attached were washed out. It can be seen in figure 15 in column day 0 after nanoparticle that the SPIONs-FA-N3 nanoparticles are far more dispersed than the SPIONs-PEG-N3-FA nanoparticles, possibly because of the PEG group on the SPIONs-PEG-N3-FA particle. This influences the attachment of the nanoparticles to the spheroid and depth that the nanoparticles go in the spheroid. The cryosection also concluded that the nanoparticles without PEG move deeper into the spheroid than the nanoparticles with PEG.

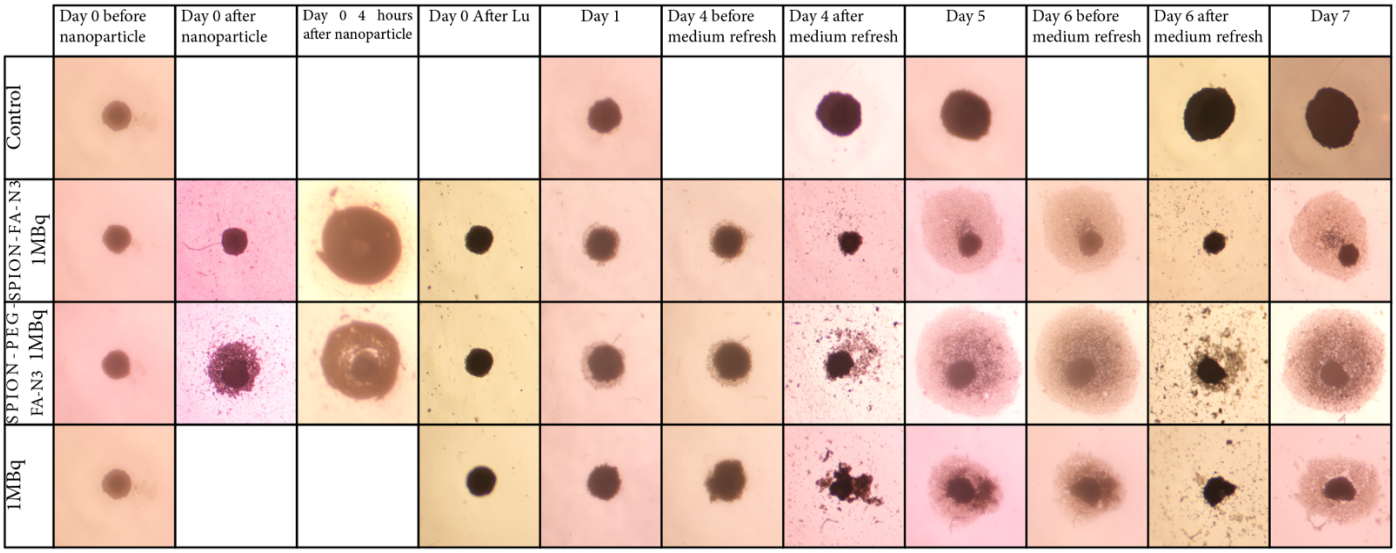

Figure 15. *Shows inverted microscope images of control spheroid and the spheroids treated with 1 MBq ^{177}Lu-DOTA-cyclooctyne taken over 7 days. Furthermore, it shows every picture of every handling (spheroid just after adding nanoparticles, spheroid after 4 hours incubation with nanoparticles, spheroid just after ^{177}Lu-DOTA-cyclooctyne treatment and the spheroids before and after medium refresh on day 4 and 7) of the spheroid and the influence of the handling. The first row shows the control spheroid, the second row the spheroid treated with nanoparticle SPIONs-FA-N3 and 1 MBq ^{177}Lu-DOTA-cyclooctyne, the third row shows the spheroid treated with nanoparticle SPIONs-PEG-N3-FA and 1 MBq Lu-177 and the last row the spheroid treated with only 1MBq ^{177}Lu-DOTA-cyclooctyne.*

4 Conclusion

The goal of this study was to observe the differences in cell uptake behavior of the SPIONs-FA-N3-FITC and SPIONs-PEG-N3-FA-FITC nanoparticles due to addition of PEG to the nanoparticles. For this purpose U87 spheroids were used to verify whether the nanoparticles are internalized by the cells. This has been done by growing U87 spheroids, incubating them with SPIONs-FA-N3-FITC and SPIONs-PEG-N3-FA-FITC nanoparticles, performing a cryosection on these spheroids, imaging the slices of the cryosection with a fluorescence microscope and analyzing the iron-content of the slices with ICP-OES.

The images of the cryosection of the spheroids that were incubated for 4 hours showed both SPIONs-FA-N3-FITC and SPIONs-PEG-N3-FA-FITC nanoparticles clustered together on the outside of the spheroid and did not diffuse further to the interior of the spheroid. A signficant difference between the two types of nanoparticles with and without PEG could not be seen. Similarly, the 24 hours incubation with both types of nanoparticles did not show significant differences in the cryosection images of the spheroids. The nanoparticles were still clustered like it the case of 4 hours incubation, with the difference that more nanoparticles were clustered and more moved inside the spheroid. Thereby, SPIONs-FA-N3-FITC nanoparticles penetrated further into the spheroid than the SPIONs-PEG-N3-FA-FITC nanoparticles. This is probably caused by the presence of PEG group. It is yet unclear from the fluorescence microscope images whether the nanoparticles are located in the exterior or taken up by the cancer cells. Further study must be done to answer this question.

From the ICP-OES it can be concluded that 4 hours incubation with both SPIONs-FA-N3-FITC and SPIONs-PEG-N3-FA-FITC nanoparticles results in 3% retention, while longer incubation for 24 hours amounts to 18% for SPIONs-FA-N3-FITC and 12% for SPIONs-PEG-N3-FA-FITC. Unfortunately, the ICP-data obtained on the cryosections cannot be used because there were too many impurities of Fe (like the marker and freezing medium), which cannot be explained yet.

The second part of the paper was the preliminary study into the click-reaction between ^{177}Lu-DOTA-cyclooctyne complex and the azide-functionalized nanoparticles SPIONs-FA-N3 and SPIONs-PEG-N3-FA. U87 spheroids were grown and incubated with nanoparticles SPIONs-FA-N3 and SPIONs-PEG-N3-FA, incubated with Lu-177-complex and observed with an inverted microscope over 7 days.

The microscope images showed that the 0.1 MBq with SPIONs-FA-N3 and SPIONs-PEG-N3-FA had no effect on the spheroids. There was no difference between the control spheroids and the spheroids treated with 0.1 MBq. It could not be seen if the click reaction between the ^{177}Lu-DOTA-cyclooctyne complex and the nanoparticles that retained on the spheroids took place. The 1 MBq dose had more damaging effect on the spheroids. The spheroids treated with nanoparticles SPIONs-FA-N3 and SPIONs-PEG-N3-F in

combination with ^{177}Lu-DOTA-cyclooctyne showed more damage to the spheroids than the spheroids only treated with ^{177}Lu-DOTA-cyclooctyne one day after the treatment. This implies that the click reaction could have taken place. However, after day 4 the spheroids showed the same amount of damage. The 30 minutes incubation of the 1MBq ^{177}Lu-DOTA-cyclooctyne was enough to do significant amount of damage with and without the click reaction.

5 Recommendations

The data obtained in this research is not conclusive for evaluation whether the nanoparticles are taken up by the cancer cells or accumulate in the outer layer of spheroids. However, small differences found for PEGylated and non-PEGylated nanoparticles suggest that it is worth further investigation. It is clear that the fluorescence microscope used in this study was not optimal. A confocal microscope with higher magnification could provide more answers to this question as it enables imaging of individual cancer cells.

Only U87 GBM cancer cell line was used in this research, it would be interesting to investigate how the nanoparticles behave with different cancer cells lines. U87 is just one of the cell lines of central nervous system cancer. The other cancer cell lines, e.g., breast, colon, kidney, leukemia, lung, melanoma, ovary, and prostate can be interesting as well due to overexpression of folate receptors. This would tell us more about the effectiveness of the nanoparticles on the different types of cancers and would be useful to know for further researching and developing the nanoparticles for a specific cancer.

To further study into the azide click reaction with ^{177}Lu-DOTA-cyclooctyne complex and the nanoparticles SPIONs-FA-N3 and SPIONs-PEG-N3-FA radioactivity lower than 1MBq should be used, because this dose seemed to be too toxic. There should also be looked into longer incubation times of the nanoparticles with the spheroid, to see if this influences the azide click reaction and the therefore the spheroid.

Bibliography

Albanese, A., Tang, P. S., & Chan, W. C. W. (2012). The Effect of Nanoparticle Size, Shape, and Surface Chemistry on Biological Systems. Annual Review of Biomedical Engineering, 14(1), 1–16. https://doi.org/10.1146/annurev-bioeng-071811-150124

American Cancer Society. Global Cancer Facts & Figures 4th Edition. Atlanta: American Cancer Society; 2018

American Cancer Society. (2014, October 27). The Science Behind Radiation Therapy. Cancer.Org. https://www.cancer.org/content/dam/CRC/PDF/Public/6151.00.pdf

Arora, M. (2013). Cell Culture Media: A Review. Materials and Methods, 3. https://doi.org/10.13070/mm.en.3.175

Arruebo, M., Vilaboa, N., Sáez-Gutierrez, B., Lambea, J., Tres, A., Valladares, M., & González-Fernández, A. (2011). Assessment of the evolution of cancer treatment therapies. Cancers, 3(3), 3279–3330. https://doi.org/10.3390/cancers3033279

Banerjee, S., Pillai, M. R. A., & Knapp, F. F. R. (2015). Lutetium-177 Therapeutic Radiopharmaceuticals: Linking Chemistry, Radiochemistry, and Practical Applications. Chemical Reviews, 115(8), 2934–2974. https://doi.org/10.1021/cr500171e

Barrow, M., Taylor, A., Fuentes-Caparrós, A. M., Sharkey, J., Daniels, L. M., Mandal, P., Park, B. K., Murray, P., Rosseinsky, M. J., & Adams, D. J. (2017). SPIONs for cell labelling and tracking using MRI: magnetite or maghemite?. Biomaterials science, 6(1), 101–106. https://doi.org/10.1039/c7bm00515f

Bionumbers. (n.d.). *Size of U87 (glioblastoma) cell - Human Homo sapiens - BNID 108941*. Size of U87 (Glioblastoma) Cell. Retrieved May 4, 2021, from https://bionumbers.hms.harvard.edu/bionumber.aspx?s=n&v=0&id=108941

Bozzuto, G., & Molinari, A. (2015). Liposomes as nanomedical devices. International Journal of Nanomedicine, 975. https://doi.org/10.2147/ijn.s68861

Breakthrough alpha-ray treatment of cancer without external radiation (2019, April 2) retrieved 6 April 2021 from https://medicalxpress.com/news/2019-04-breakthrough-alpha-ray-treatment-cancer-external.html

Bresciani, G., Hofland, L. J., Dogan, F., Giamas, G., Gagliano, T., & Zatelli, M. C. (2019). Evaluation of Spheroid 3D Culture Methods to Study a Pancreatic Neuroendocrine Neoplasm Cell Line. Frontiers in Endocrinology, 10. https://doi.org/10.3389/fendo.2019.00682

Clark, M. J., Homer, N., O'Connor, B. D., Chen, Z., Eskin, A., Lee, H., Merriman, B., & Nelson, S. F. (2010). U87MG decoded: the genomic sequence of a cytogenetically aberrant human cancer cell line. PLoS genetics, 6(1), e1000832. https://doi.org/10.1371/journal.pgen.1000832

D'Alessio, A., Proietti, G., Sica, G., & Scicchitano, B. M. (2019). Pathological and Molecular Features of Glioblastoma and Its Peritumoral Tissue. Cancers, 11(4), 469. https://doi.org/10.3390/cancers11040469

de Kruijff, R. M., Wolterbeek, H. T., & Denkova, A. G. (2015). A Critical Review of Alpha Radionuclide Therapy-How to Deal with Recoiling Daughters?. Pharmaceuticals (Basel, Switzerland), 8(2), 321–336. https://doi.org/10.3390/ph8020321

Dolgin, E. (2016). Venerable brain-cancer cell line faces identity crisis. Nature, 537(7619), 149–150. https://doi.org/10.1038/nature.2016.20515

Dulińska-Litewka, J., Łazarczyk, A., Hałubiec, P., Szafrański, O., Karnas, K., & Karewicz, A. (2019). Superparamagnetic Iron Oxide Nanoparticles—Current and Prospective Medical Applications. Materials, 12(4), 617. https://doi.org/10.3390/ma12040617

Emmett, L., Willowson, K., Violet, J., Shin, J., Blanksby, A., & Lee, J. (2017). Lutetium177PSMA radionuclide therapy for men with prostate cancer: a review of the current literature and discussion of practical aspects of therapy. Journal of Medical Radiation Sciences, 64(1), 52–60. https://doi.org/10.1002/jmrs.227

Gal, N., Lassenberger, A., Herrero-Nogareda, L., Scheberl, A., Charwat, V., Kasper, C., & Reimhult, E. (2017). Interaction of Size-Tailored PEGylated Iron Oxide Nanoparticles with Lipid Membranes and Cells. ACS Biomaterials Science & Engineering, 3(3), 249–259. https://doi.org/10.1021/acsbiomaterials.6b00311

Herranz, F., Morales, M. P., Roca, A. G., Vilar, R., & Ruiz-Cabello, J. (2008). A new method for the aqueous functionalization of superparamagnetic Fe2O3nanoparticles. Contrast Media & Molecular Imaging, 3(6), 215–222. https://doi.org/10.1002/cmmi.254

Hobro, A. J., & Smith, N. I. (2017). An evaluation of fixation methods: Spatial and compositional cellular changes observed by Raman imaging. Vibrational Spectroscopy, 91, 31–45. https://doi.org/10.1016/j.vibspec.2016.10.012

Huang, C., Neoh, K. G., & Kang, E.-T. (2011). Combined ATRP and 'Click' Chemistry for Designing Stable Tumor-Targeting Superparamagnetic Iron Oxide Nanoparticles. Langmuir, 28(1), 563–571. https://doi.org/10.1021/la202441j

Hur, W., & Yoon, S. (2017). Molecular Pathogenesis of Radiation-Induced Cell Toxicity in Stem Cells. International Journal of Molecular Sciences, 18(12), 2749. https://doi.org/10.3390/ijms18122749

Khanna, S., Chauhan, A., Bhatt, A. N., & Dwarakanath, B. S. R. (2020). Multicellular tumor spheroids as in vitro models for studying tumor responses to anticancer therapies. Animal Biotechnology, 251–268. https://doi.org/10.1016/b978-0-12-811710-1.00011-2

Knight, J. C., & Cornelissen, B. (2014). Bioorthogonal chemistry: implications for pretargeted nuclear (PET/SPECT) imaging and therapy. American journal of nuclear medicine and molecular imaging, 4(2), 96–113.

Kucheryavykh, Y. V., Davila, J., Ortiz-Rivera, J., Inyushin, M., Almodovar, L., Mayol, M., Morales-Cruz, M., Cruz-Montañez, A., Barcelo-Bovea, V., Griebenow, K., & Kucheryavykh, L. Y. (2019). Targeted Delivery of Nanoparticulate Cytochrome C into Glioma Cells Through the Proton-Coupled Folate Transporter. Biomolecules, 9(4), 154. https://doi.org/10.3390/biom9040154

Kumari, P., Ghosh, B., & Biswas, S. (2015). Nanocarriers for cancer-targeted drug delivery. Journal of Drug Targeting, 24(3), 179–191. https://doi.org/10.3109/1061186x.2015.1051049

Lassenberger, A., Scheberl, A., Stadlbauer, A., Stiglbauer, A., Helbich, T., & Reimhult, E. (2017). Individually Stabilized, Superparamagnetic Nanoparticles with Controlled Shell and Size Leading to Exceptional Stealth Properties and High Relaxivities. *ACS Applied Materials & Interfaces*, *9*(4), 3343–3353. https://doi.org/10.1021/acsami.6b12932

Low, P. S., & Kularatne, S. A. (2009). Folate-targeted therapeutic and imaging agents for cancer. Current Opinion in Chemical Biology, 13(3), 256–262. https://doi.org/10.1016/j.cbpa.2009.03.022

Majkowska-Pilip, A., Gawęda, W., Żelechowska-Matysiak, K., Wawrowicz, K., & Bilewicz, A. (2020). Nanoparticles in Targeted Alpha Therapy. Nanomaterials (Basel, Switzerland), 10(7), 1366. https://doi.org/10.3390/nano10071366

Milla, P., Dosio, F., & Cattel, L. (2012). PEGylation of Proteins and Liposomes: a Powerful and Flexible Strategy to Improve the Drug Delivery. Current Drug Metabolism, 13(1), 105–119. https://doi.org/10.2174/138920012798356934

Mohapatra, A., Uthaman, S., & Park, I.-K. (2019). Polyethylene Glycol Nanoparticles as Promising Tools for Anticancer Therapeutics. Polymeric Nanoparticles as a Promising Tool for Anti-Cancer Therapeutics, 205–231. https://doi.org/10.1016/b978-0-12-816963-6.00010-8

Nunes, A. S., Barros, A. S., Costa, E. C., Moreira, A. F., & Correia, I. J. (2018). 3D tumor spheroids as in vitro models to mimic in vivo human solid tumors resistance to therapeutic drugs. Biotechnology and Bioengineering, 116(1), 206–226. https://doi.org/10.1002/bit.26845

Pearce, A. K., & O'Reilly, R. K. (2019). Insights into Active Targeting of Nanoparticles in Drug Delivery: Advances in Clinical Studies and Design Considerations for Cancer Nanomedicine. Bioconjugate Chemistry, 30(9), 2300–2311. https://doi.org/10.1021/acs.bioconjchem.9b00456

Pinto, B., Henriques, A. C., Silva, P. M. A., & Bousbaa, H. (2020). Three-Dimensional Spheroids as In Vitro Preclinical Models for Cancer Research. Pharmaceutics, 12(12), 1186. https://doi.org/10.3390/pharmaceutics12121186

Poty, S., Mandleywala, K., O'Neill, E., Knight, J. C., Cornelissen, B., & Lewis, J. S. (2020). 89Zr-PET imaging of DNA double-strand breaks for the early monitoring of response following α- and β-particle radioimmunotherapy in a mouse model of pancreatic ductal adenocarcinoma. Theranostics, 10(13), 5802–5814. https://doi.org/10.7150/thno.44772

Ramil, C. P., & Lin, Q. (2013). Bioorthogonal chemistry: strategies and recent developments. Chemical Communications, 49(94), 11007. https://doi.org/10.1039/c3cc44272a

Revia, R. A., & Zhang, M. (2016). Magnetite nanoparticles for cancer diagnosis, treatment, and treatment monitoring: recent advances. Materials Today, 19(3), 157–168. https://doi.org/10.1016/j.mattod.2015.08.022

Sollini, M., Marzo, K., Chiti, A. et al. The five “W”s and “How” of Targeted Alpha Therapy: Why? Who? What? Where? When? and How?. Rend. Fis. Acc. Lincei 31, 231–247 (2020). https://doi.org/10.1007/s12210-020-00900-2

Souster, E., Goodwin, V., Jackson, A., Beaver, C., Behan, F., Ansari, R., & Garnett, M. (2020). Passaging adherent cancer cell lines v1 (protocols.io.bgtbjwin). Protocols.Io. Published. https://doi.org/10.17504/protocols.io.bgtbjwin

Stéen, E. J. L., Edem, P. E., Nørregaard, K., Jørgensen, J. T., Shalgunov, V., Kjaer, A., & Herth, M. M. (2018b). Pretargeting in nuclear imaging and radionuclide therapy: Improving efficacy of theranostics and nanomedicines. Biomaterials, 179, 209–245. https://doi.org/10.1016/j.biomaterials.2018.06.021

Sung, H., Ferlay, J., Siegel, R. L., Laversanne, M., Soerjomataram, I., Jemal, A., & Bray, F. (2021). Global cancer statistics 2020: GLOBOCAN estimates of incidence and mortality worldwide for 36 cancers in 185 countries. CA: A Cancer Journal for Clinicians, 1. https://doi.org/10.3322/caac.21660

Tchoryk, A., Taresco, V., Argent, R. H., Ashford, M., Gellert, P. R., Stolnik, S., Grabowska, A., & Garnett, M. C. (2019). Penetration and Uptake of Nanoparticles in 3D Tumor Spheroids. *Bioconjugate Chemistry*, *30*(5), 1371–1384. https://doi.org/10.1021/acs.bioconjchem.9b00136

Thermo Fischer 1. (n.d.). Balanced Salt Solutions | Thermo Fisher Scientific - NL. Balanced Salt Solutions. Retrieved May 4, 2021, from https://www.thermofisher.com/nl/en/home/life-science/cell-culture/mammalian-cell-culture/reagents/balancedsaltsolutions.html?ef_id=Cj0KCQjw4cOEBhDMARIsAA3XDRju2zluf7BvCiBNkeeILrQYVkWOGAv6boiaiYd2yiBpmmuu0VMkF38aAlNEALw_wcB:G:s&s_kwcid=AL!3652!3!391186515055!b!!g!!%2Bpbs%20%2Bcell%20%2Bculture&cid=bid_clb_cce_r01_co_cp0000_pjt0000_bid00000_0se_gaw_nt_pur_con&gclid=Cj0KCQjw4cOEBhDMARIsAA3XDRju2zluf7BvCiBNkeeILrQYVkWOGAv6boiaiYd2yiBpmmuu0VMkF38aAlN-EALw_wcB

Thermo Fischer 2. (n.d.). PANC-1 Cell Line Spheroid Generation for HT Assays | Thermo Fisher Scientific - NL. Retrieved May 9, 2021, from https://www.thermofisher.com/nl/en/home/references/protocols/cell-culture/3-d-cell-culture-protocol/panc1-cell-line-spheroid-generation.html

Urbańska, K., Sokołowska, J., Szmidt, M., & Sysa, P. (2014). Glioblastoma multiforme - an overview. Contemporary oncology (Poznan, Poland), 18(5), 307–312. https://doi.org/10.5114/wo.2014.40559

WHO. Cancer. (2021, March 3). https://www.who.int/news-room/fact-sheets/detail/cancer. Accessed on 15 march 2021

Zwicke, G. L., Mansoori, G. A., & Jeffery, C. J. (2012). Utilizing the folate receptor for active targeting of cancer nanotherapeutics. Nano reviews, 3, 10.3402/nano.v3i0.18496. https://doi.org/10.3402/nano.v3i0.18496

Appendix A

Spheroid treated with SPIONs-FA-N3-FITC nanoparticle for 4h, the diameter of this spheroid was 431 µm

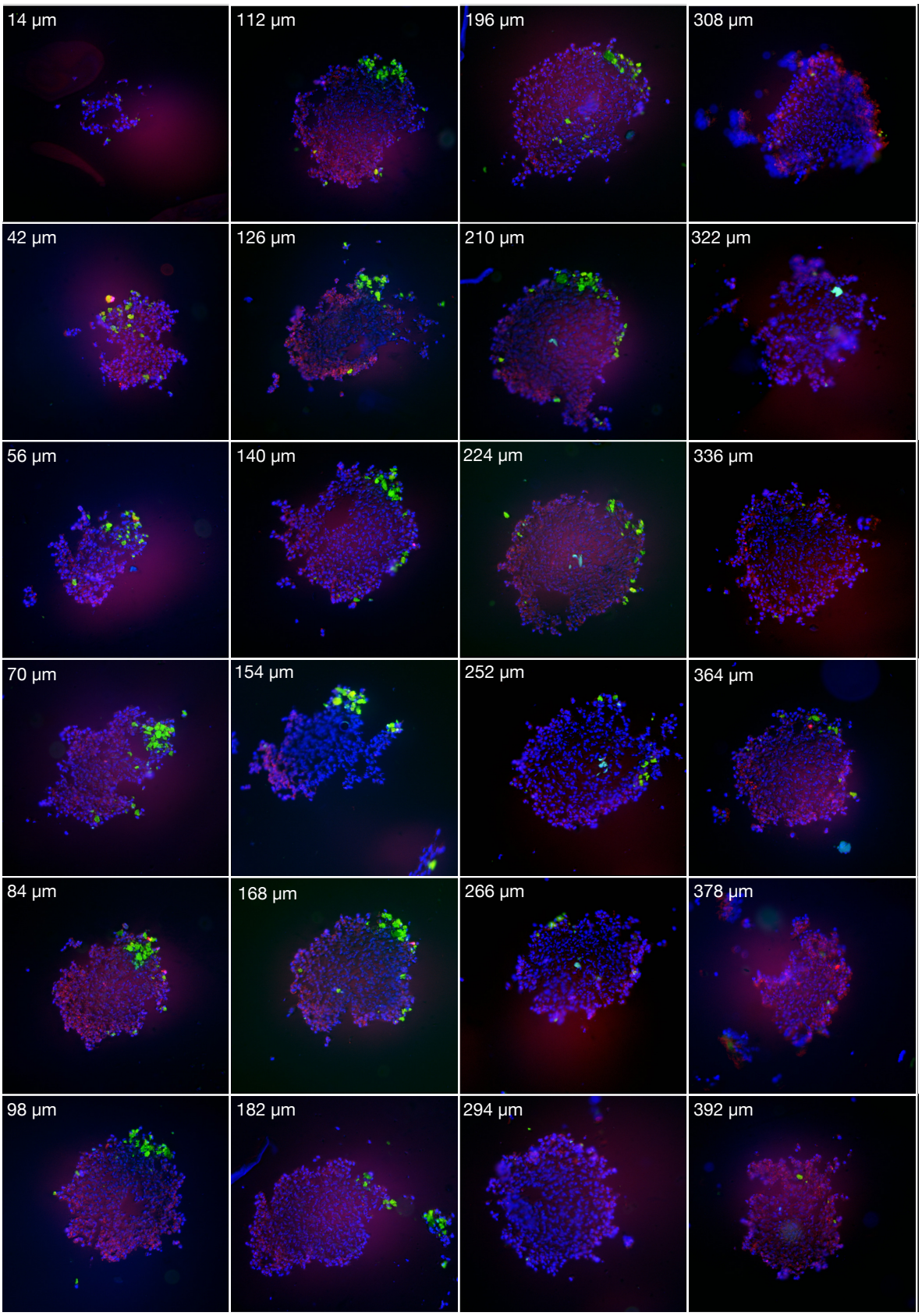

Spheroid treated with SPIONs-FA-N3-FITC nanoparticle for 24h, the diameter of this spheroid was 431 µm

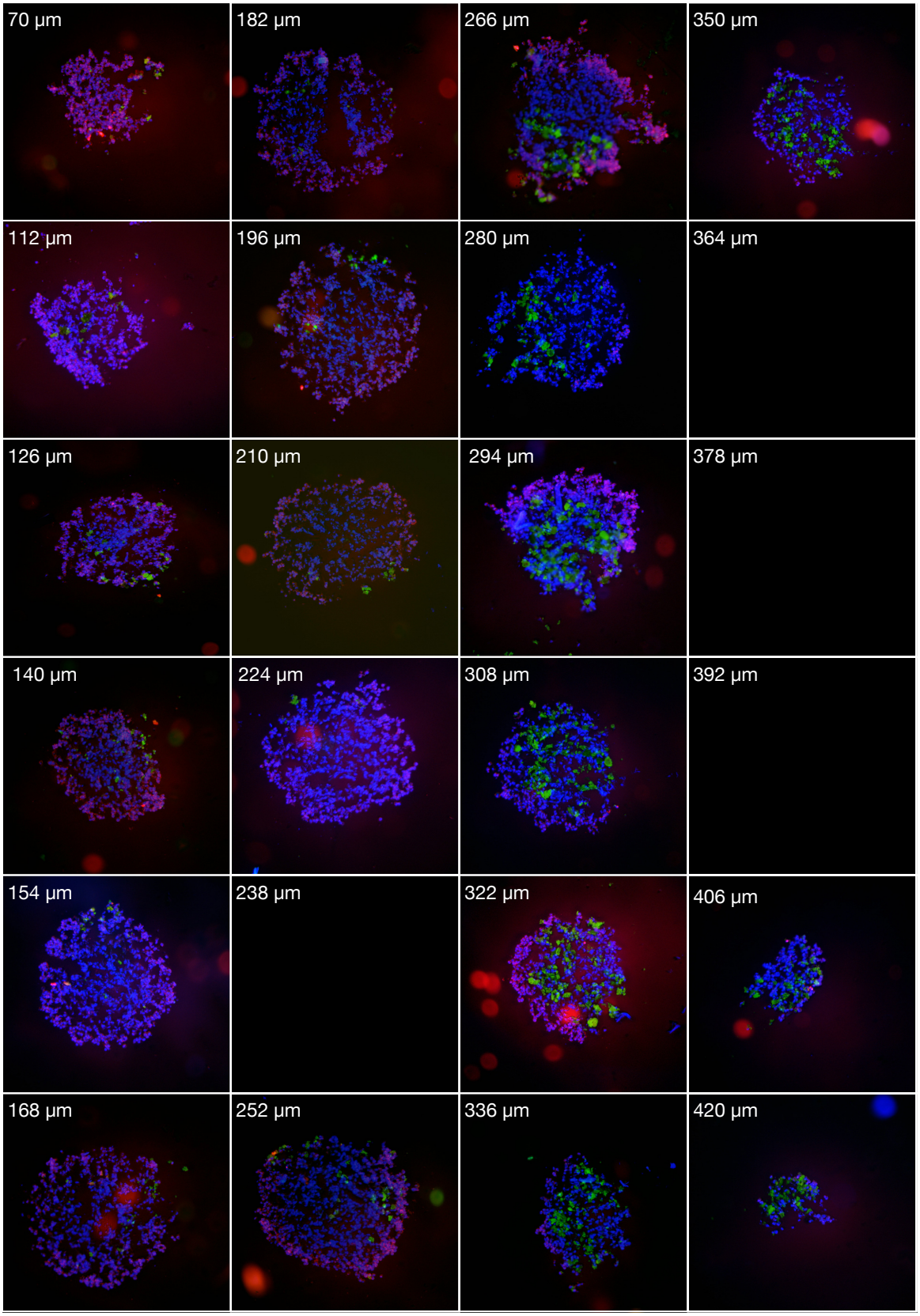

Spheroid treated with SPIONs-PEG-N3-FA-FITC nanoparticle for 4h, the diameter of this spheroid was 431 µm

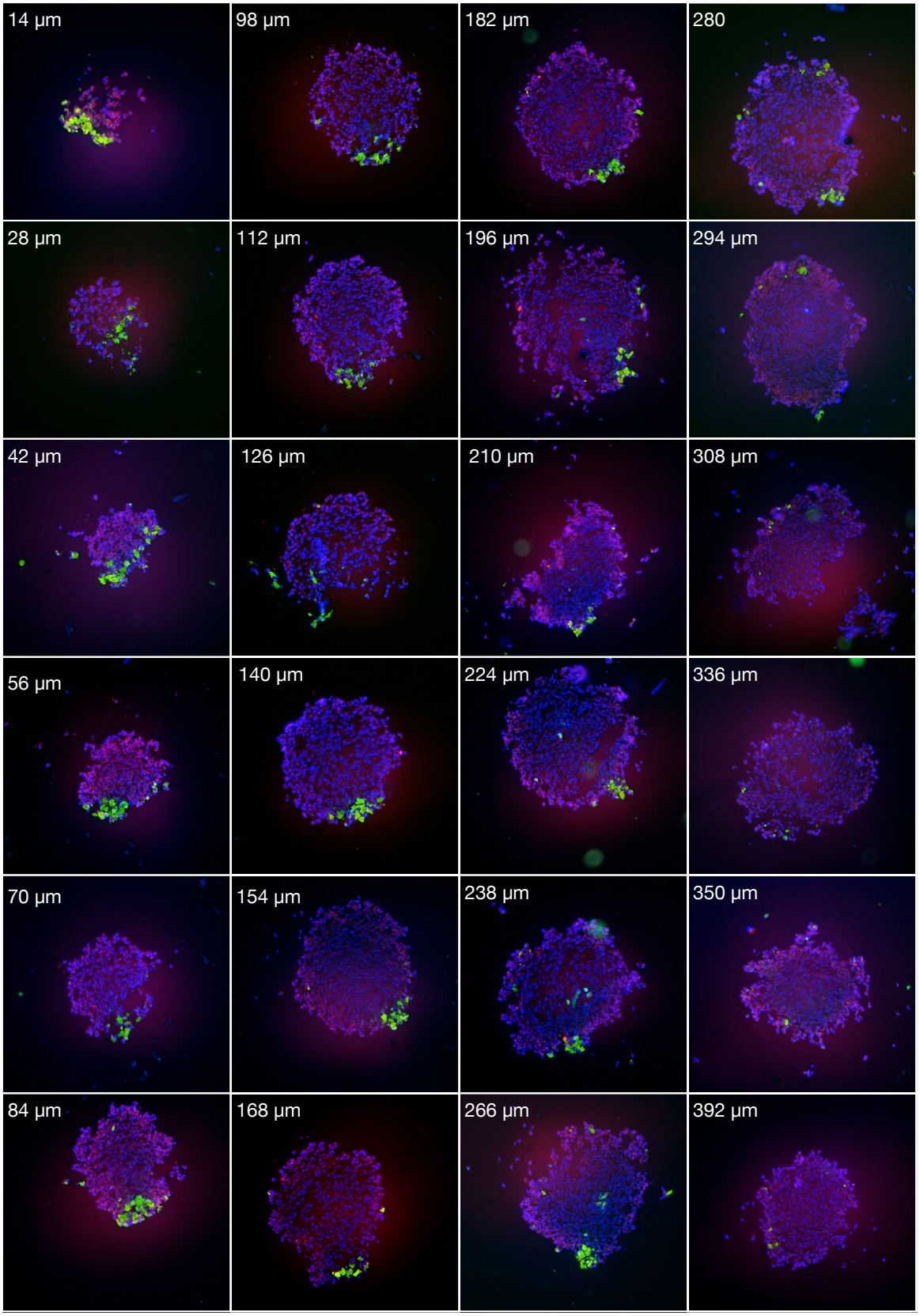

Spheroid treated with SPIONs-PEG-N3-FA-FITC nanoparticle for 24h, the diameter of this spheroid was 431 µm